

Structural Analysis of Large Caliber Hybrid Ceramic/Steel Gun Barrels

MS Thesis

Jon DeLong

*Department of Mechanical Engineering
Clemson University*

OUTLINE

- **Merger of ceramics into the conventional steel gun barrel design**
- **Use of a probabilistic structural analysis to understand residual stress development in shrink-fit process**
 - **Probabilistic structural analysis combined with Mean Value Method**
 - **Adaptive Importance Sampling**
- **Reliability analysis of hybrid barrels to assess the risk of rupture**
 - **Use of internal ballistic codes to determine the thermal boundary and initial conditions**
 - **Use of Weibull's Weakest Link Theory and Principle of Independent Action to determine the ceramic reliability**

**Merger of Ceramics into
the Conventional Steel
Gun Barrel Design**

Need for Performance Enhancements in Conventional Large Caliber Guns

- **Increased Range with Accuracy**
- **Increased Energy-on-target**

Favorable Ceramic Properties:

- **High Melting Temperature**
- **High Hot Hardness**
- **Chemical Inertness**

Limited Experimental Investigations into Ceramic Linings Concluded

- SiC, Si₃N₄, and SiAlON survived 1,000 single shots & 100 burst fired rounds
- Circumferential crack formation and growth at barrel ends

Reasons for Ceramic Lining Failure

- Shrink-fit process induces a triaxial compressive stress state in liner
- Relaxation of compressive stress causes slippage at liner/jacket interface near barrel ends

Part I

Use of Probabilistic Structural Analysis to Understand Residual Stress Development

Probabilistic Structural Analysis

Limit-State Function Concept

$$g(\mathbf{X}) = Z(\mathbf{X}) - z_0 = 0$$

$$\mathbf{X} = (X_1, X_2, \dots, X_n)$$

Failure Region $\sim g(x) \leq 0$

Safe Region $\sim g(x) > 0$

$Z(\mathbf{X}) \rightarrow$ Performance Function

$z_0 \rightarrow$ Critical Value

Probability of Failure

$$P_f = \int \dots \int_{\Omega} f_x(X') dX'$$

Ω denotes the failure domain

- Extremely difficult to solve for complicated failure functions but can be straightforward using Monte Carlo methods
 - Random sampling of each design variable according to its distribution followed by evaluation of the performance
 - Repeat procedure until large numbers of $Z(x)$ values can give the statistics of the response
- Strength is that it is exact in the limit of a large sample #'s
- Weakness is that a very large number of functional evaluations may be necessary

Advanced Mean Value Method (AMV)

Bridge between crude Mean Value (MV) and Monte Carlo method based on Cumulative Distribution Function (CDF)

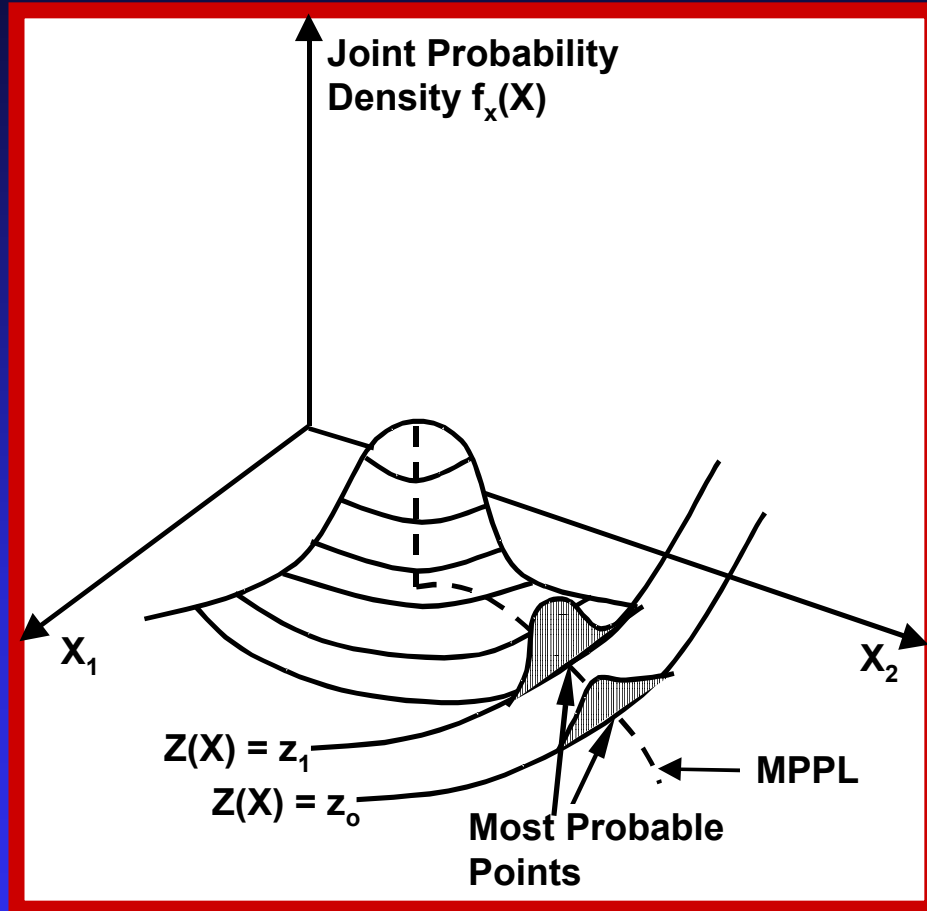
For MV, begin with truncated Taylor Series

$$Z_{MV} = Z(\mu_x) + \sum_{i=1}^n \left(\frac{\partial Z}{\partial X_i} \right) \cdot (X_i - \mu_i) = a_0 + \sum_{i=1}^n a_i X_i$$

AMV

$$Z_{AMV} = Z_{MV} + H(Z_{MV})$$

- $H(Z_{MV})$ is **NEGATIVE** difference between Z_{MV} and $Z(X)$ along the Most Probable Point (MPP) locus
- MPP is the point with the max joint probability density



(MPP)

- To find MPP locus solve optimization problem:
- $\min |u|$ subject to $Z(u) = z_0$
- when $\min |u|$ is determined it becomes u^* and the corresponding variable in the X-space becomes X^*

- With ALL variables converted to standard normal variables $Z(X)$ is converted to $Z(u)$
- MPP in u -space for $Z(u) = z_0$ is point defined on the limit state surface $g(u) = Z(u) - z_0$ closest to the origin

- The accuracy of the AMV solution depends on the accuracy of the MPP locus
- Further improvements on the solution can be made

AMV+

- Repeat AMV procedure, now around the MPP
- Use Taylor series approximation

$$Z_{MPP} = Z(X^*) + \sum_{i=1}^n \left(\frac{\partial Z}{\partial X_i} \right) \cdot (X_i - x^*_i) = b_0 + \sum_{i=1}^n b_i X_i$$

- This equation becomes constraint equation in optimization
- MPP is then updated in the u -and X-space and variables are renamed u^{**} and X^{**}

AMV+

Number of function evaluations in method

Purpose	MV	AMV	AMV+
To Develop an MV-based Linearized Response Function, Z_{MV}	n+1	n+1	n+1
To Compute the System Response at the MPP for a Selected Level of CDF		+1	+1
To Develop an MPP-based Linearized Response Function, Z_{MPP}			+n+1
Total Number of Function Evaluations	n+1	n+2	2n+3

Adaptive Importance Sampling

- Minimizes safe region sampling, focuses on failure
- Sampling region boundary continuously deformed until region completely covers failure region

$$g_s(\mathbf{u}) = \nabla g_s(\mathbf{u}^*)^T (\mathbf{u} - \mathbf{u}^*) + \frac{1}{2} (\mathbf{u} - \mathbf{u}^*)^T \mathbf{D}(\mathbf{u}^*) (\mathbf{u} - \mathbf{u}^*)$$

$$D_{ij}(\mathbf{u}^*) = \frac{\partial^2 g_s(\mathbf{u}^*)}{\partial u_i \partial u_j}$$



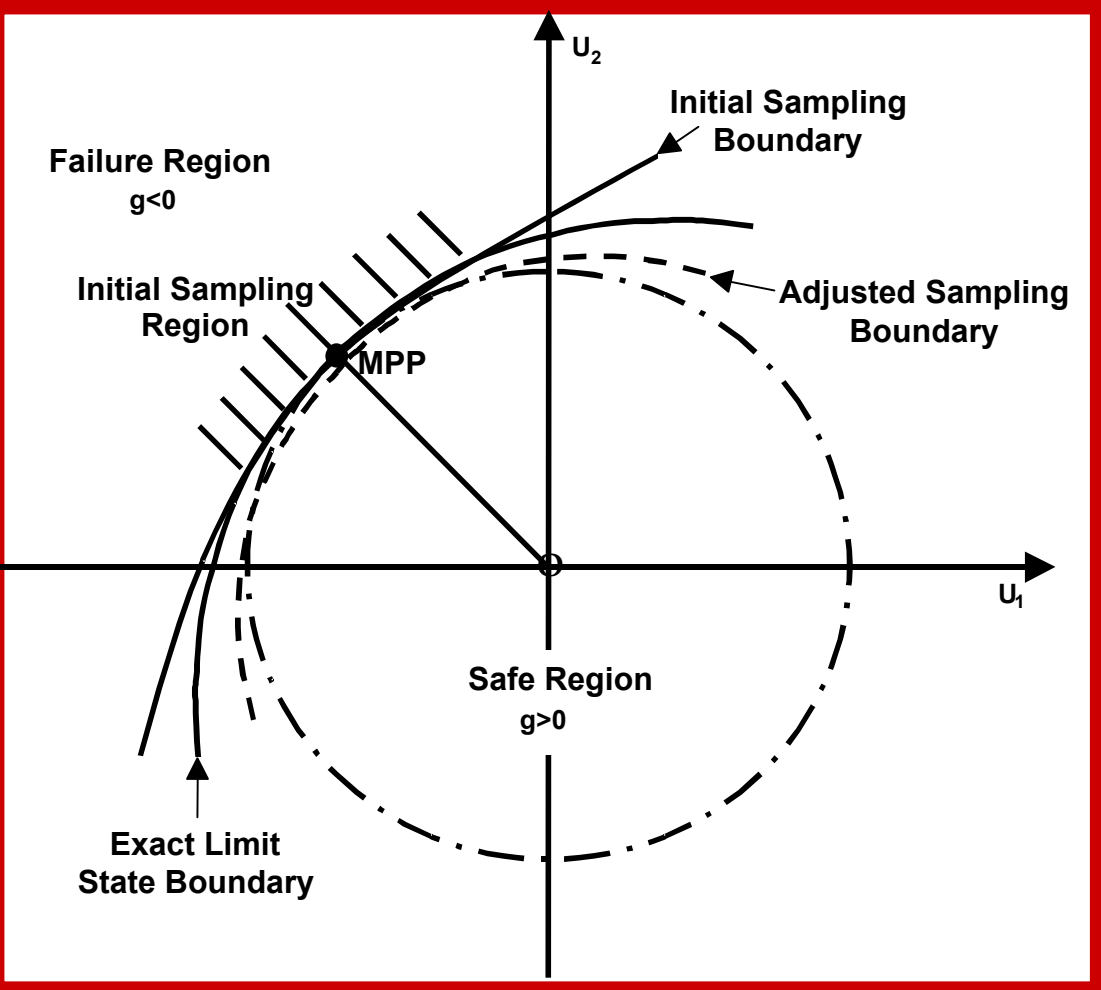
computed using finite difference and FEA evaluations

$$\mathbf{u} = -\mathbf{H}^T \mathbf{v}$$

\mathbf{H} matrix contains sensitivity factors evaluated at \mathbf{u}^*

AIS

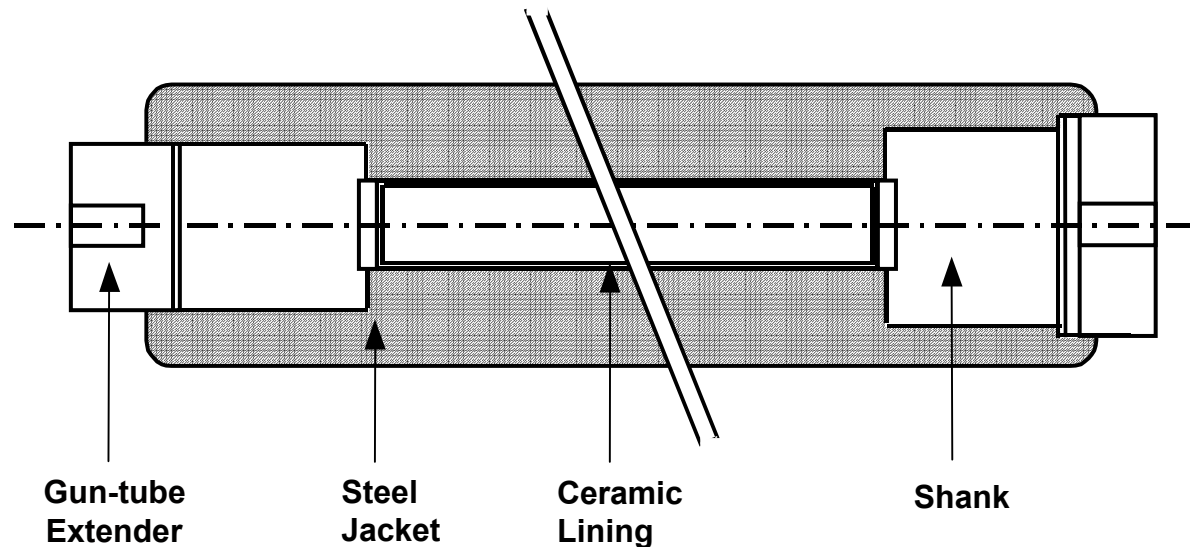
- Sampling region is transformed to align v_n with vector connecting the space origin and the MPP
- $v_i = 0$ and $v_n = \beta$
- With new coordinate system, curvature of sampling boundary can be deformed
- Realign CS with new MPP and repeat until failure probability converges



Finite Element Analysis

- Ceramic lining
 - 3.175 mm thick
- Steel Jacket
 - 25.4 mm thick

- Barrel geometry
 - 355.6 mm long
 - 25.0 mm bore



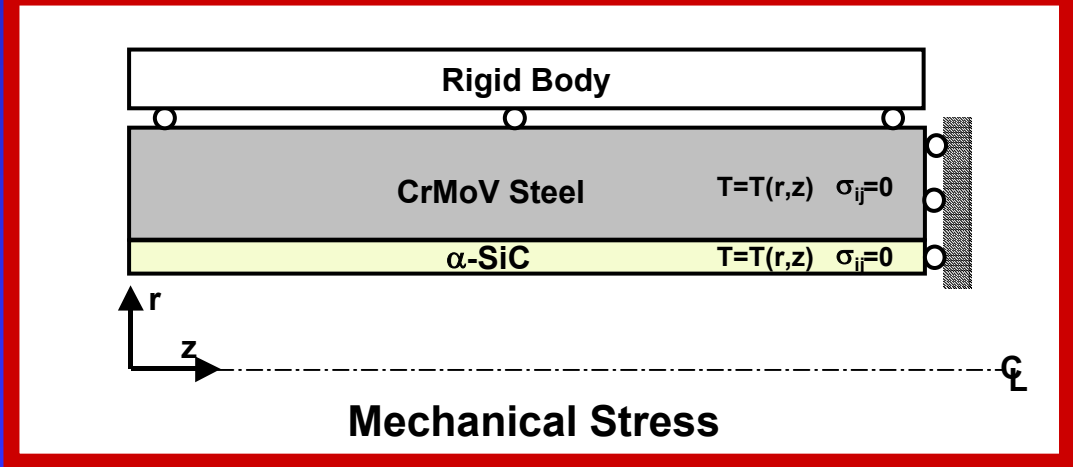
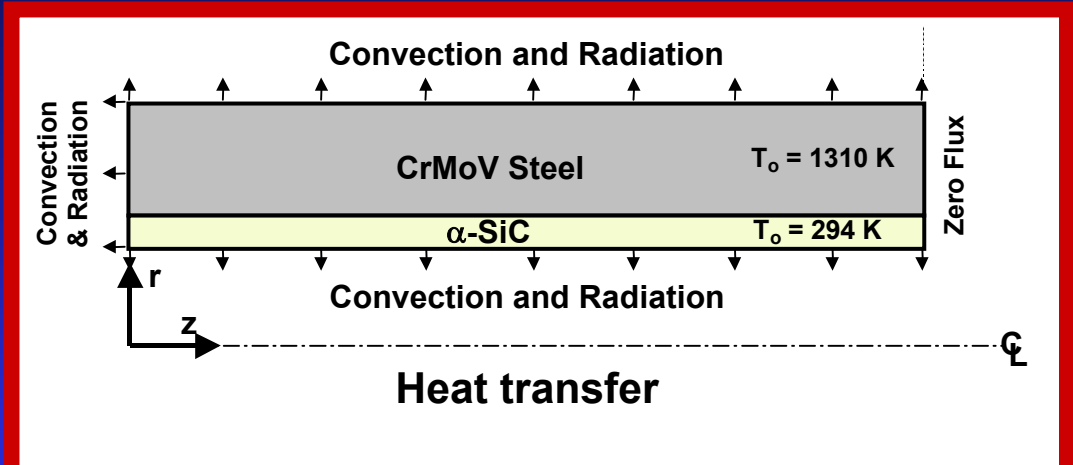
Problem Description

- Hybrid barrel formed by shrink-fit process
 - Jacket heated significantly
 - Liner OD larger than jacket ID
 - Liner develops compressive residual stresses

- Design goal is to maximize compressive stress in ceramic liner
- Problems with achieving goal
 - High tensile contact stresses at interface lead to crack formation in lining
 - Max shrink-fit temperature must not cause changes in steel microstructure

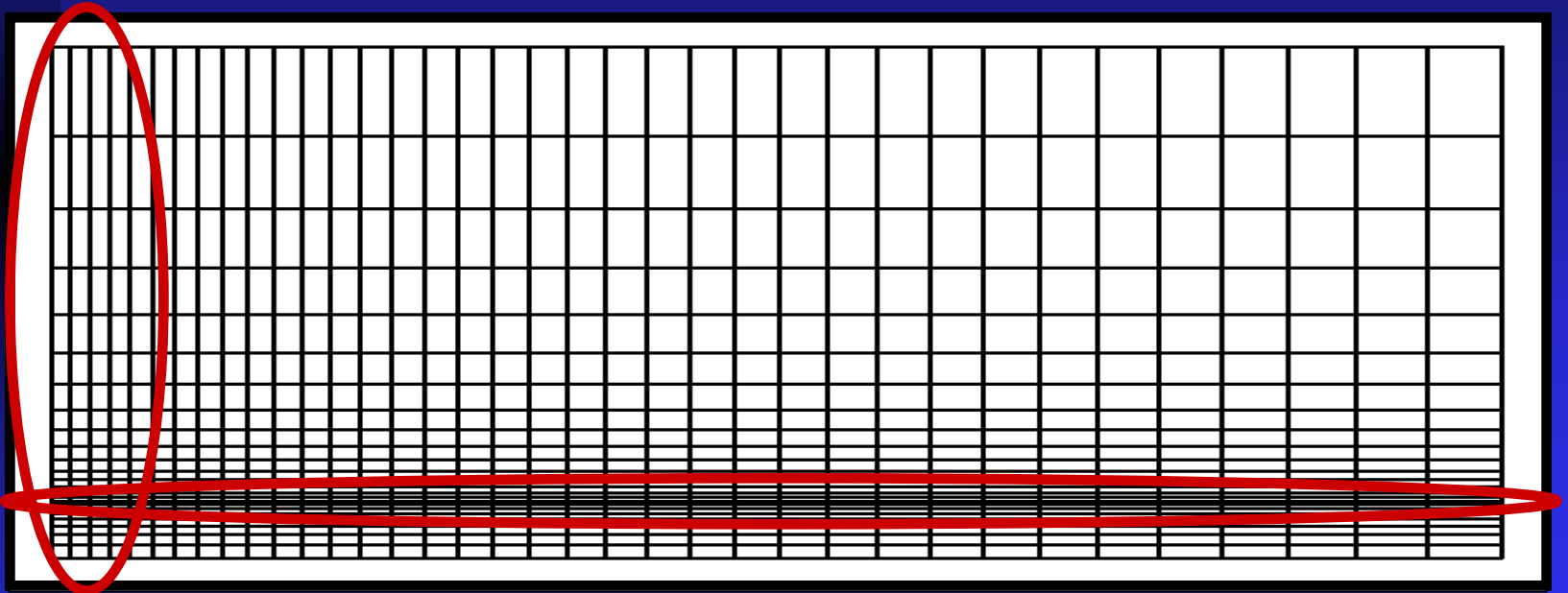
Problem Formulation

- 2 step analysis
 - Transient heat transfer
 - Elastic-plastic mechanical stress



Abaqus Mesh

152.4 mm long because of
barrel symmetry



Mesh refinement for
localized residual stress

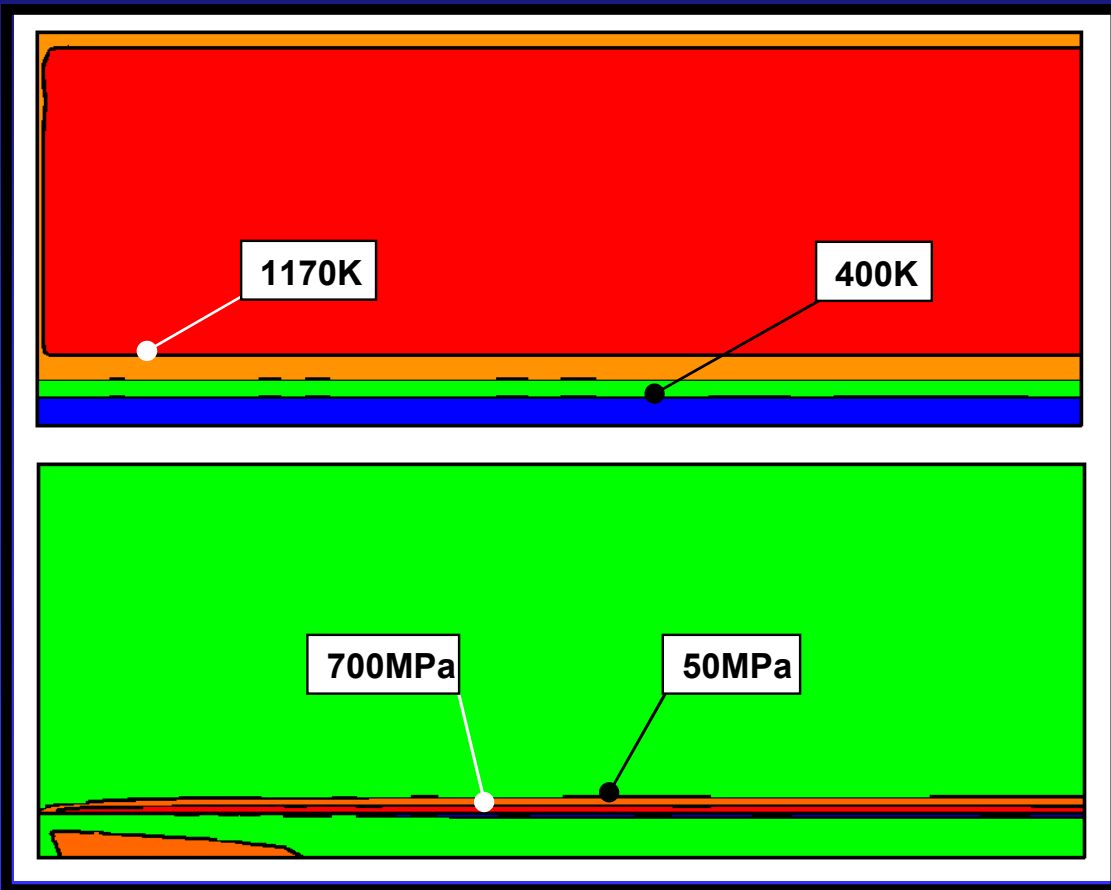
864 8-node quadrilateral
axisymmetric elements

Properties & Parameters

Property	Symbol	Unit	Material			
			α -SiC		CrMoV	
			Mean	Std. Dev.	Mean	Std. Dev.
Density	ρ	kg/m^3	3,170.0	50.0	7,850.0	50.0
Specific Heat	c_p	$J/kg \cdot K$	890.0	55.0	463.0	21.0
Thermal Conductivity	k	$W/m \cdot K$	134.0	26.0	54.6	5.5
Convective Heat Transfer Coefficient	h	$W/m^2 \cdot K$	135.0	22.0	190.0	14.0
Emissivity	ϵ	$N/$	0.82	0.07	0.55	0.12
Coefficient of Linear Thermal Expansion	α	$10^{-6} / K$	3.7	0.2	14.2	0.7
Young's Modulus	E	GPa	415.0	25.0	210.0	2.5
Poisson's Ratio	ν	N/A	0.21	0.02	0.290	0.003
Tensile Strength	σ_f	MPa	700.0	0.0*	1,070.0	70.0
α -SiC/CrMoV Steel Friction Coefficient	μ	N/A	0.3	0.1	0.3	0.1
Initial Temperature	T_0	K	298.0	0.0*	1,173.0	15.0

Mean Value Results

1 second during shrink fit process

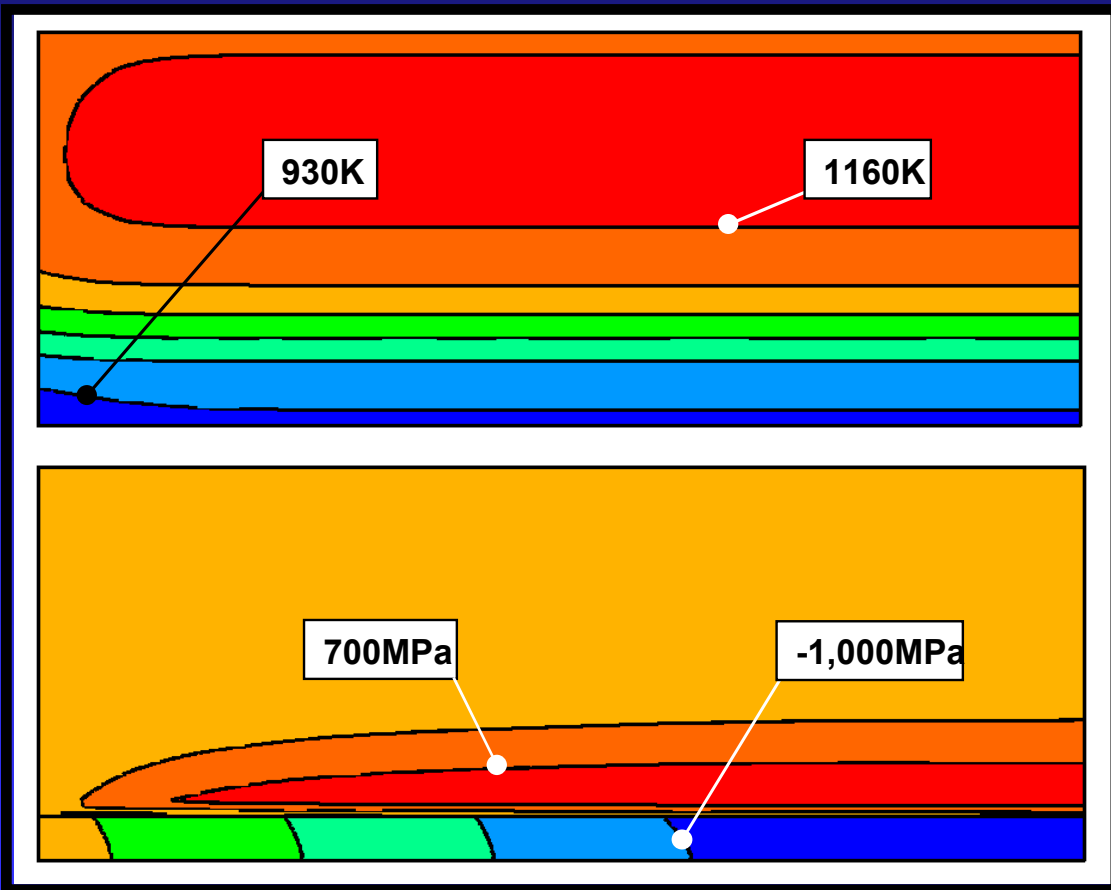


Temperature contour

Axial stress contour

Mean Value Results

10 seconds during shrink fit process

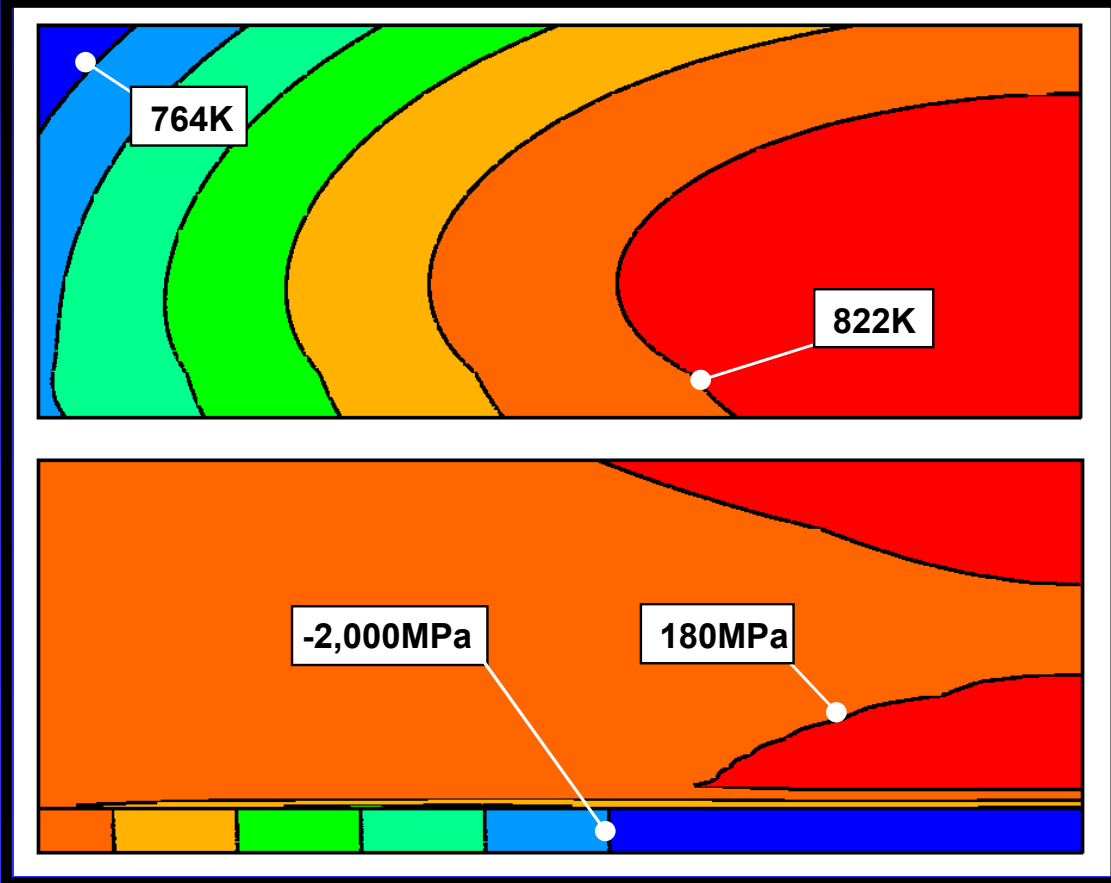


Temperature contour

Axial stress contour

Mean Value Results

100 seconds during shrink fit process



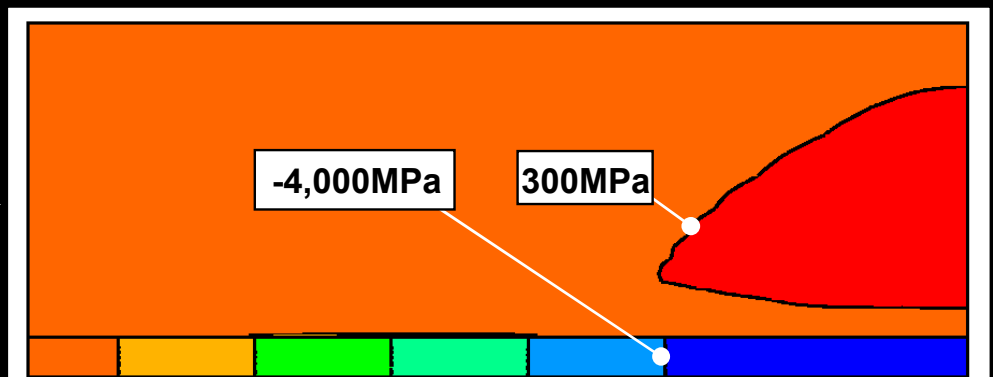
Temperature contour

Axial stress contour

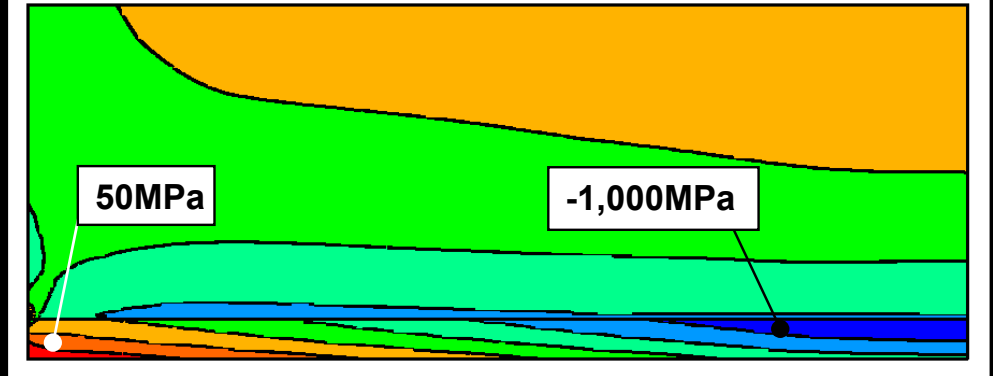
Mean Value Results

At completion of shrink fit process

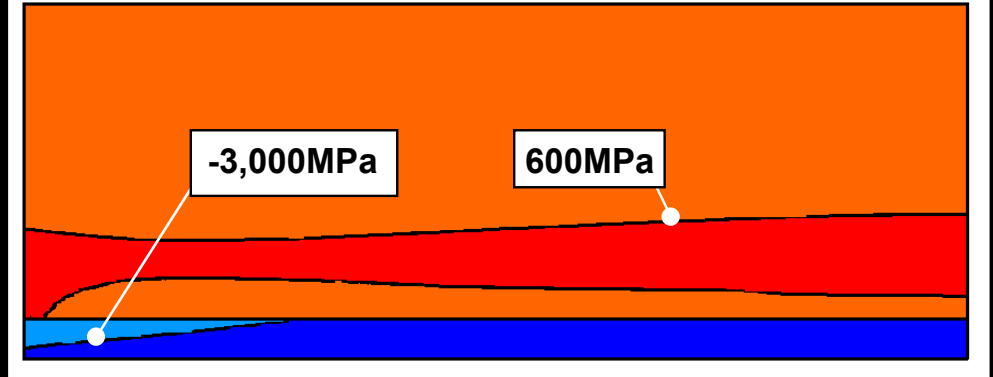
σ_{zz}



σ_{rr}

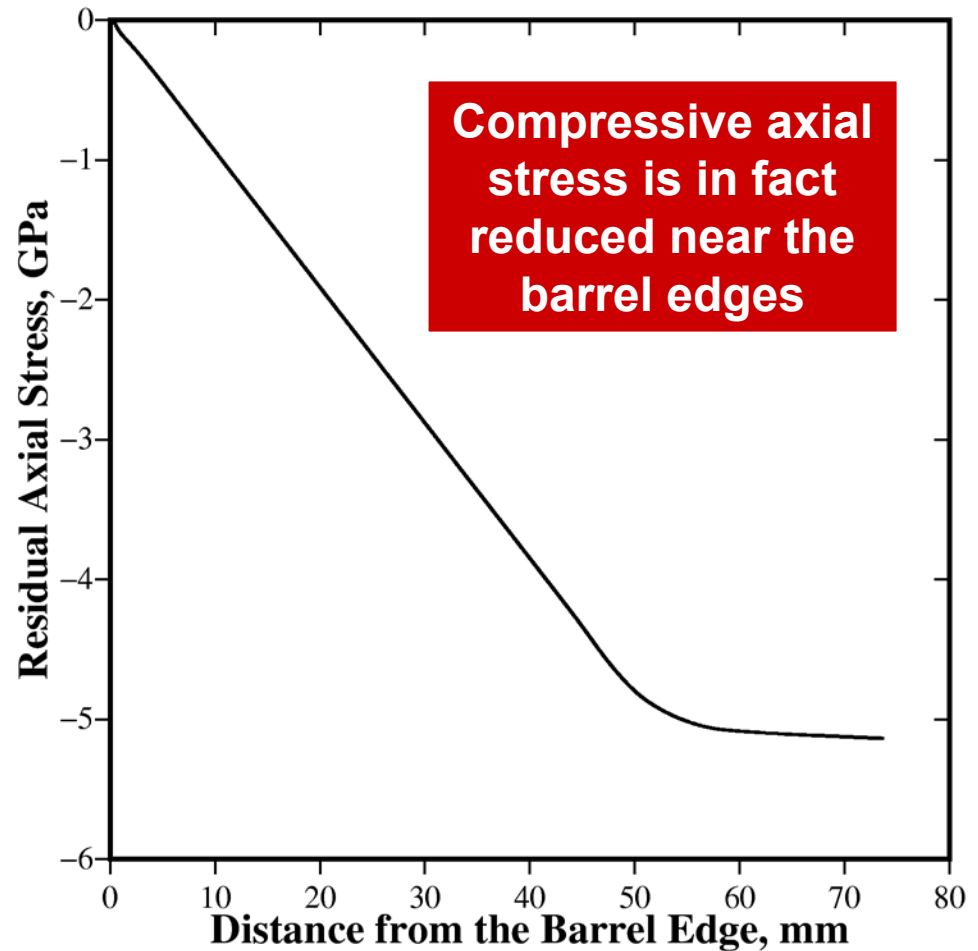


$\sigma_{\theta\theta}$



Residual Stress Variation

Stress observed in the lining at the lining/jacket interface

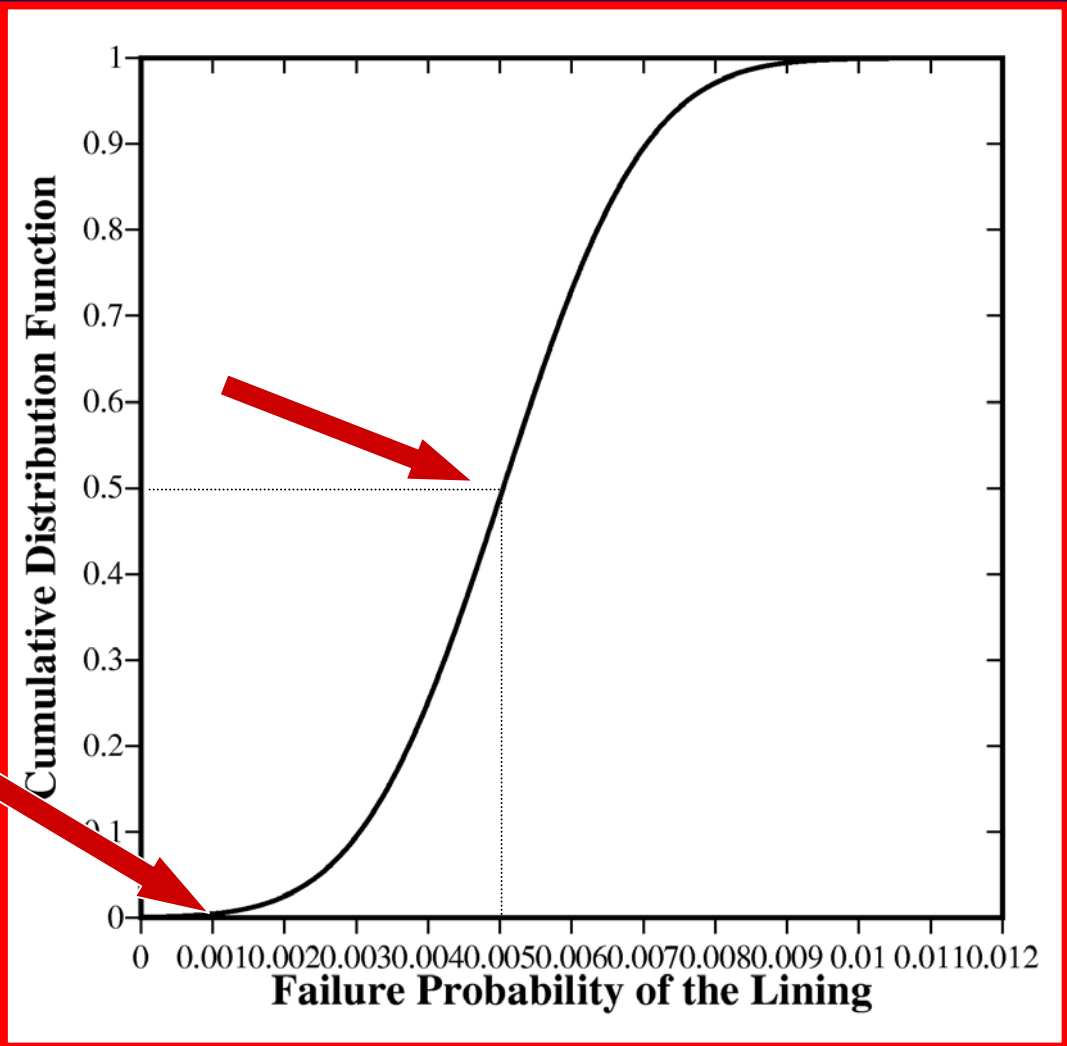


CDF

At mean values
(CDF = 0.5)
Probability for failure is ~ 0.005

Probability for no failure is ~ 0.0009

Limiting value is
 $P(x) = 0.01$



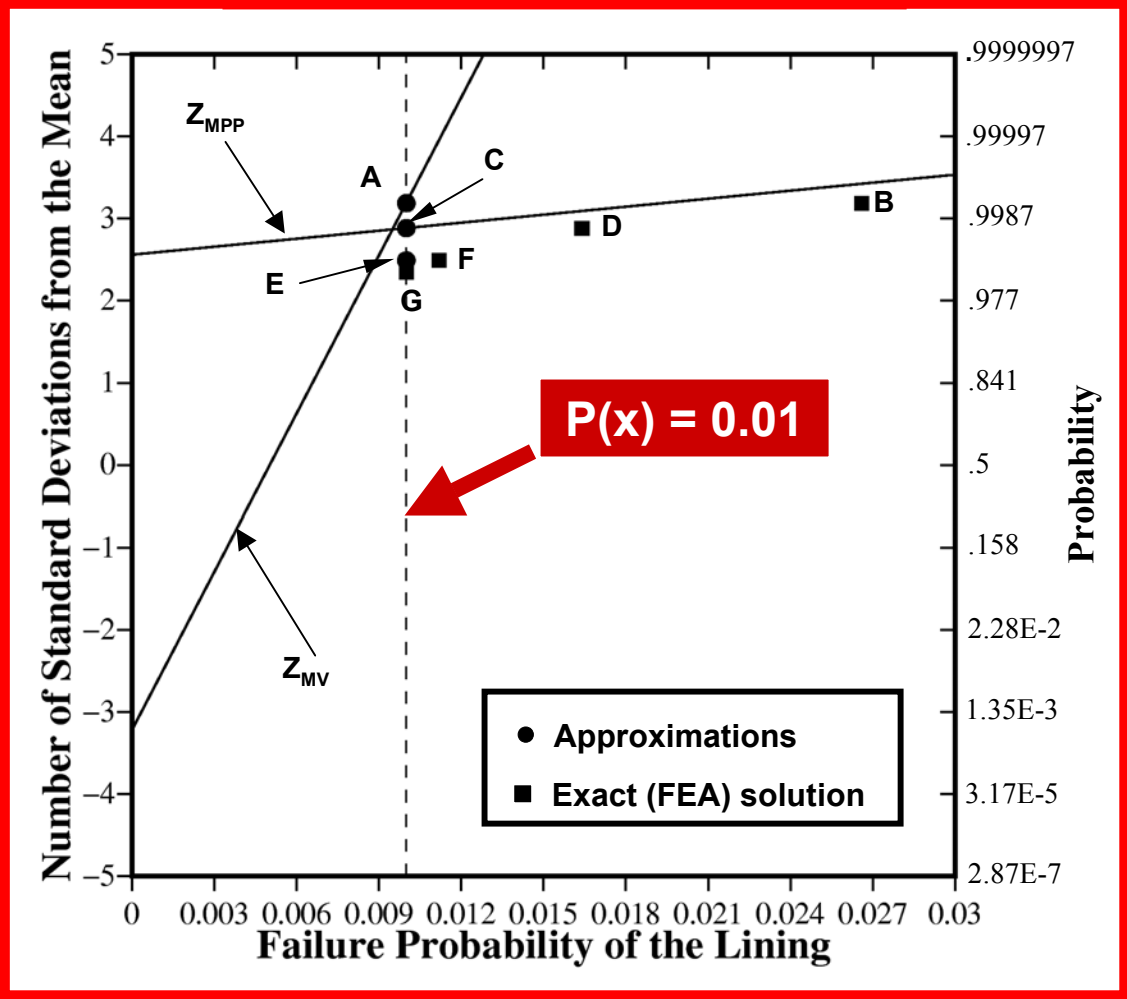
CDF

- A-MV
- B-FEA@MPP
- C-AMV+
- D-FEA@MPP#2
- E-AMV+#2
- F-FEA@MPP#3
- G-AMV+#3

Linear Nature of Z_{MV} proves normal distribution

Point "A" has a MV probability of 0.9992 (.0008)

Point "G" has a MV probability of 0.9936 (.0064)



Sampling Validation

Each Standard normal variable is perturbed around MPP (“G”) and AIS employed

- Failure probability based on PDF calculated to be 0.0079
- 10 points were sampled in order to give 18 standard normal variables with failure probability of 0.0071
- Procedure repeated with more points until the probability converged
- convergence made at 0.00688 which agrees with AMV+ solution of 0.0064

Summary of Probability Analysis

- As a result of shrink-fit, lining develops triaxial compressive residual stress but relaxes at interface near barrel ends
- Relaxation increases failure probability by increasing chance for crack growth and formation
- AMV+ and AIS methods do model the failure probability accurately with less computational effort

Part II

Reliability Analysis of Hybrid Ceramic/Steel Gun Barrels

Internal Ballistic Analysis

- **During firing cycle interior barrel wall surface heats significantly due to forced convection
 - hot combustion gases
 - friction
 - obatur galling**
- **Radiation significant at breech end of the barrel**

Film Temperature

XKTC input parameters

- Propellant microstructure
- Rheological properties
- Charge and igniter properties
- Barrel parameters
- Air shock parameters
- Projectile parameters

XKTC Code

- 1-D lumped parameter internal ballistic code
- based on conservation of mass, momentum, and energy
- considers effects of propellant properties and behavior on flow resistance
- makes allowances for non-uniformity in flow area, pressure waves, and drag

XKTC output

- Temporal and spatial history of gas temperature
- Gas pressure
- Gas velocity

Heat Transfer Coefficient

XBR-2D Calculations

$$h = 0.037 \frac{\mu^*}{x} Re^{*0.8} C_{fn} C_p$$

$$\mu^* = \frac{1.492 \cdot 10^6 T^{*1.5}}{145.8 + T^*}$$

$$Re^* = \frac{x \rho u}{\mu^*}$$

$$C_f = C_{fn} \left[1 + (\gamma - 1)^2 M^2 \right]^{-0.6}$$

$$M = \frac{u}{\sqrt{\gamma R_g T_g}}$$

XBR-2D Code

- Compressible turbulent boundary layer model
- Pressure, velocity, and temperature data from XKTC are the inputs
- Considers effects of propellant properties and behavior on flow resistance
- Makes allowances for non-uniformity in flow area, pressure waves, and drag

Reliability Analysis

$$P_{fV} = 1 - \exp\left[-\int_V N_V(\sigma)dV\right] = 1 - \exp[-B_V]$$

$$N_V(\sigma) = \left(\frac{\sigma - \sigma_{uV}}{\sigma_{oV}}\right)^{m_V}$$

- Ceramic can not redistribute high loads and local stresses induced by flaws
- Weakest Link concept used to represent ceramic components
- Size not orientation of flaw is considered

Approaches

Normal stress averaging

$$P_{fV} = 1 - \exp\left(-\int_V \left(\frac{\bar{\sigma}}{\sigma_{opV}}\right)^{m_V} dV\right)$$

$$\bar{\sigma}_o^{m_V} = \frac{\int_A \sigma_n^{m_V}}{\int_A dA}$$

Integration performed over
a tensile normal stress

Principle of Independent Action

$$P_{fV} = 1 - \exp\left[\int_V \left(\frac{\sigma_1^{m_V} + \sigma_2^{m_V} + \sigma_3^{m_V}}{\sigma_{oV}^{m_V}}\right) dV\right]$$

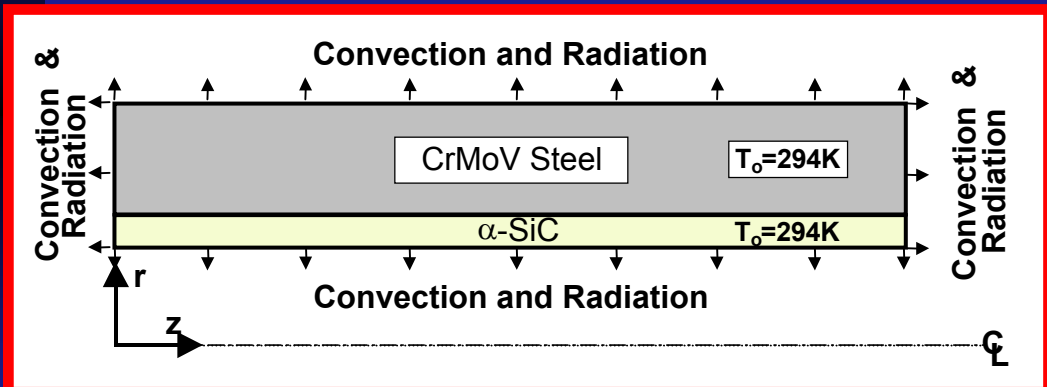
Only tensile principle stresses are considered

Problem Description

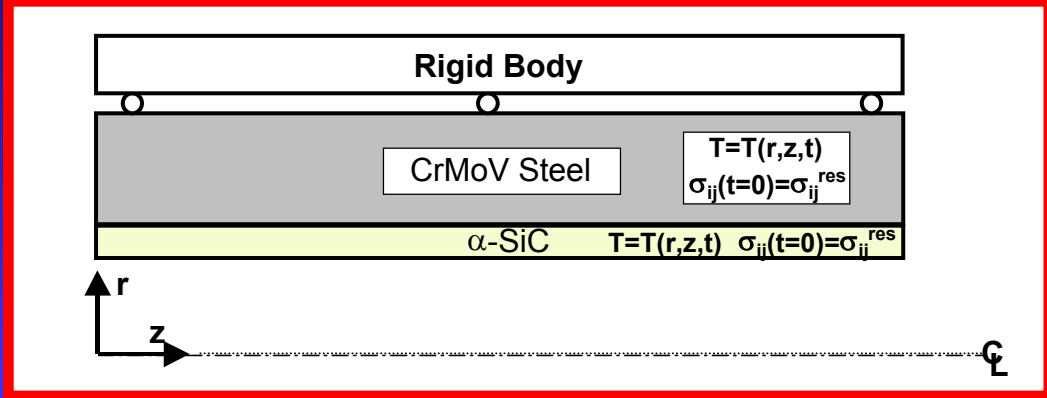
- **Barrel is subject to 2 firing modes**
 - **Single shot & burst firing**
- **Barrel has initial compressive residual stresses resulting from shrink-fit process**
 - **Too much relaxation of stress during firing is fatal**
- **Ceramic liner MUST remain compressive at the jacket/liner interface to prevent slippage**

Problem Formulation

- 2 step analysis
 - Transient heat transfer
 - Elastic-plastic mechanical stress

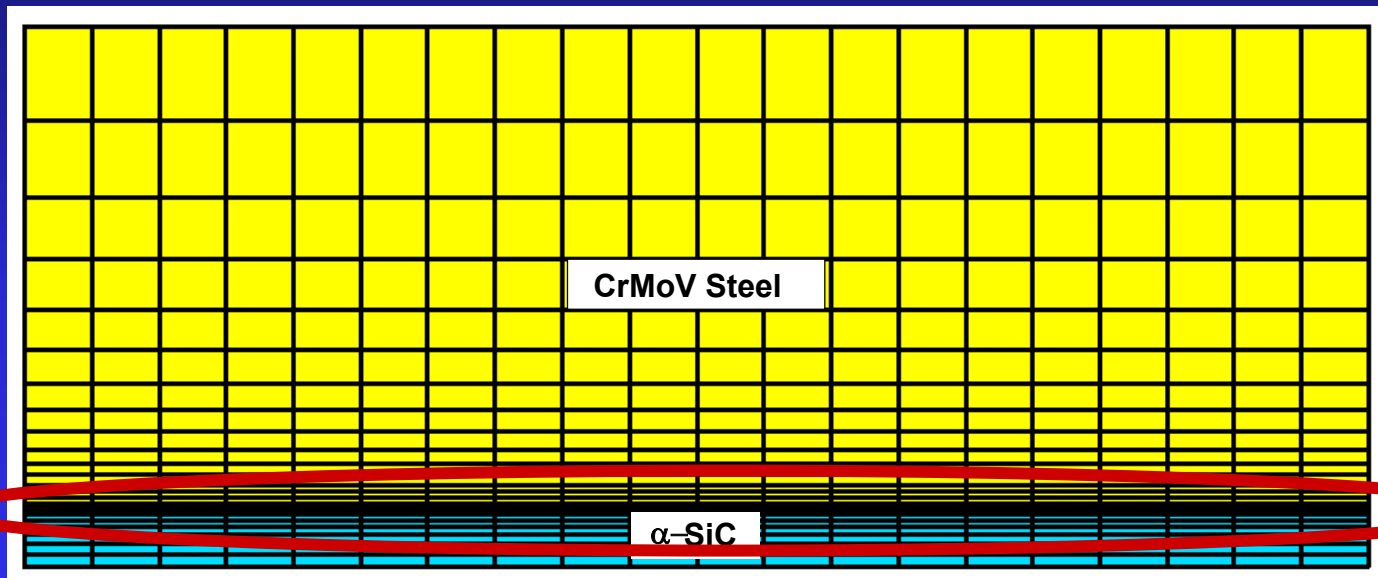


Temperature and heat transfer coefficient evolve temporally along inner barrel wall



Abaqus Mesh

2400 8-node quadrilateral
axisymmetric elements



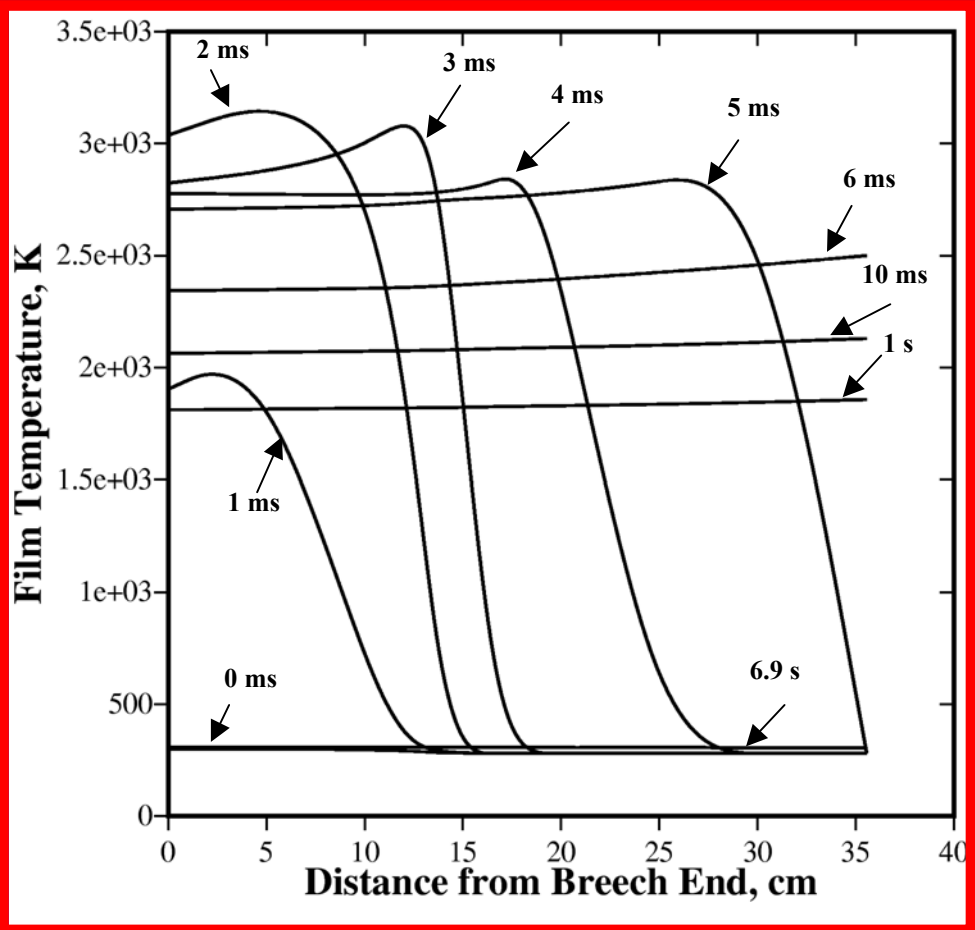
Mesh refinement for
localized residual stress

1 row of membrane
elements in liner at interface

Film Temperature Variation

Takes 5ms for heat wave to travel the barrel length

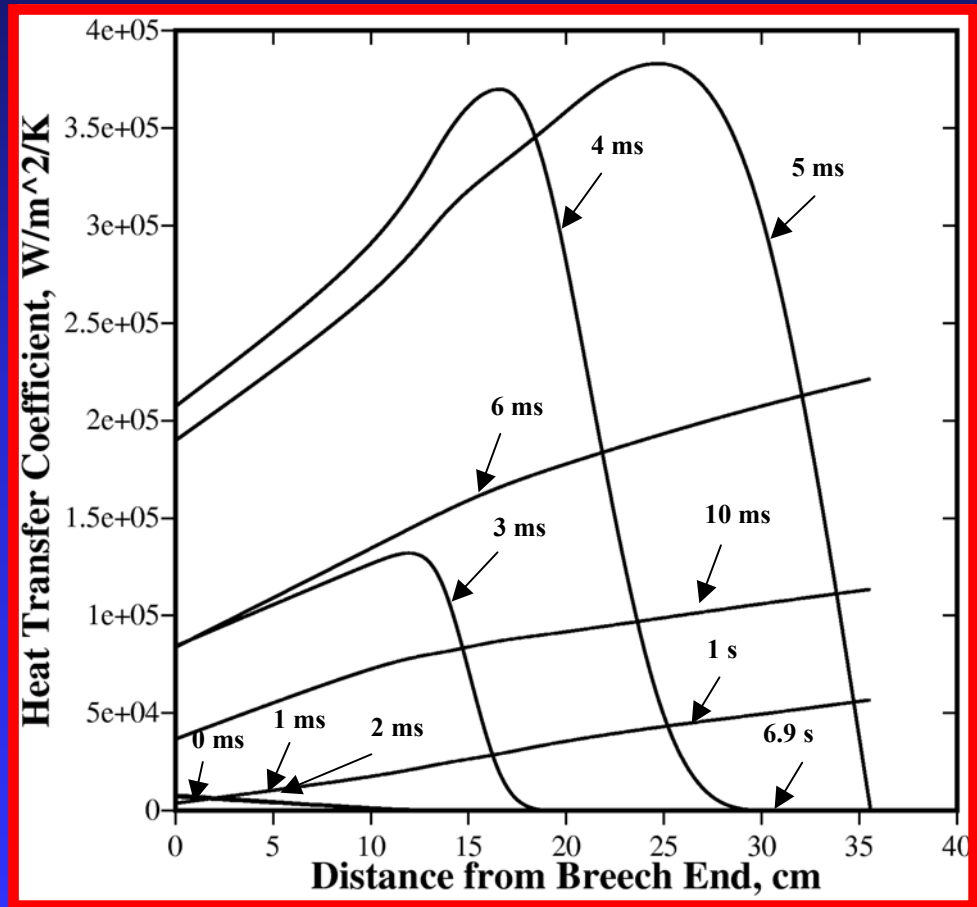
After 6ms film temperature distribution is uniform and decreases monotonically



Heat Transfer Coefficient

Takes 2ms for forced convection heat transfer coefficient to deviate from its natural convection coefficient

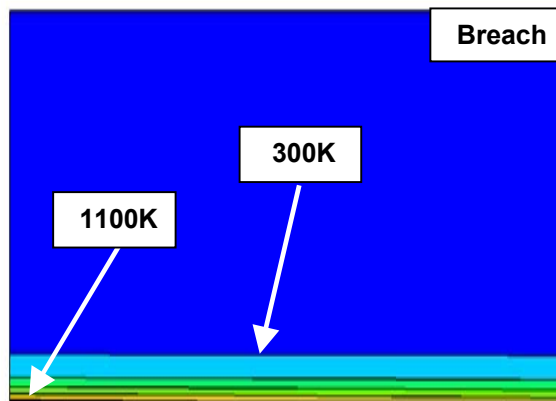
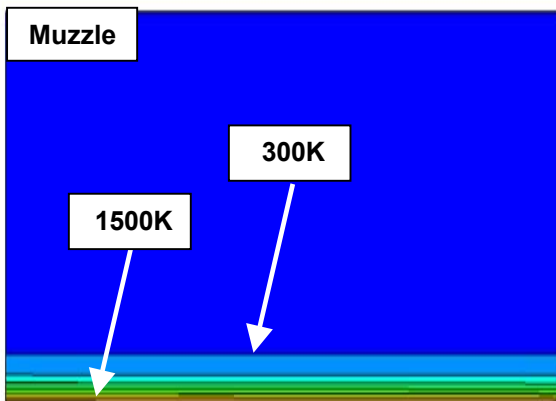
Large variation especially at 5ms



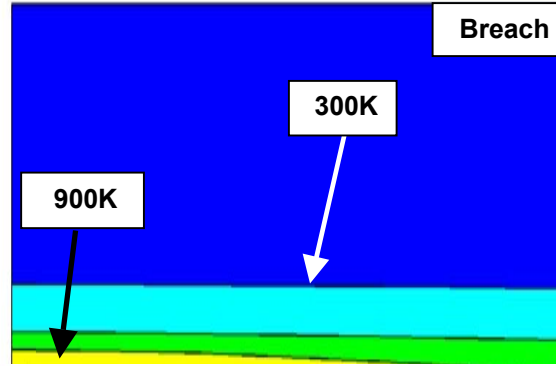
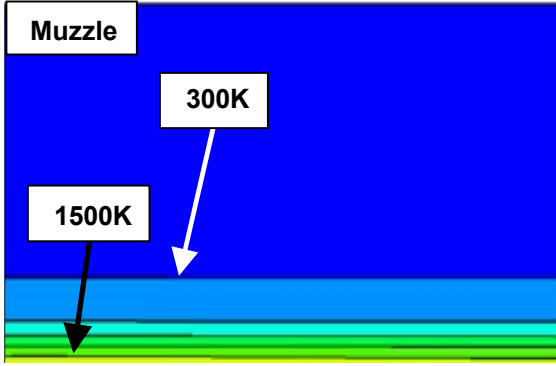
Single-shot Temperature

**Biot
Number
170**

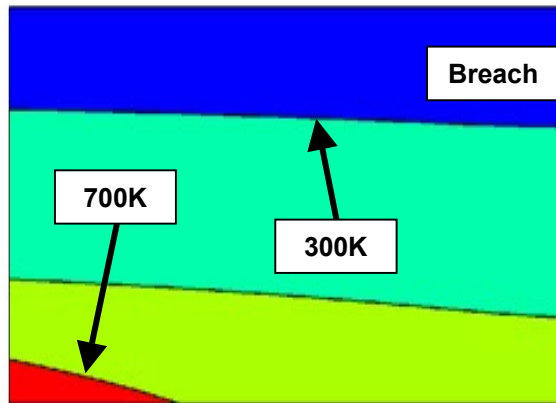
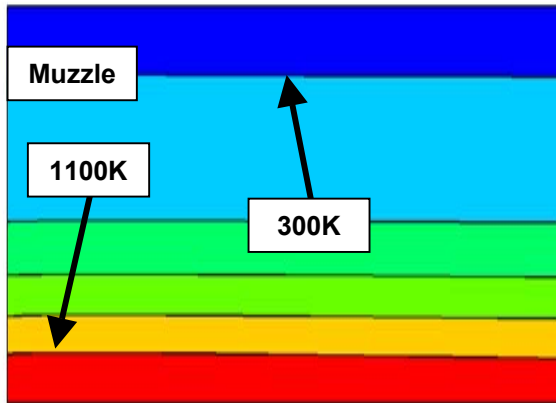
t=0.03s



t=0.3s

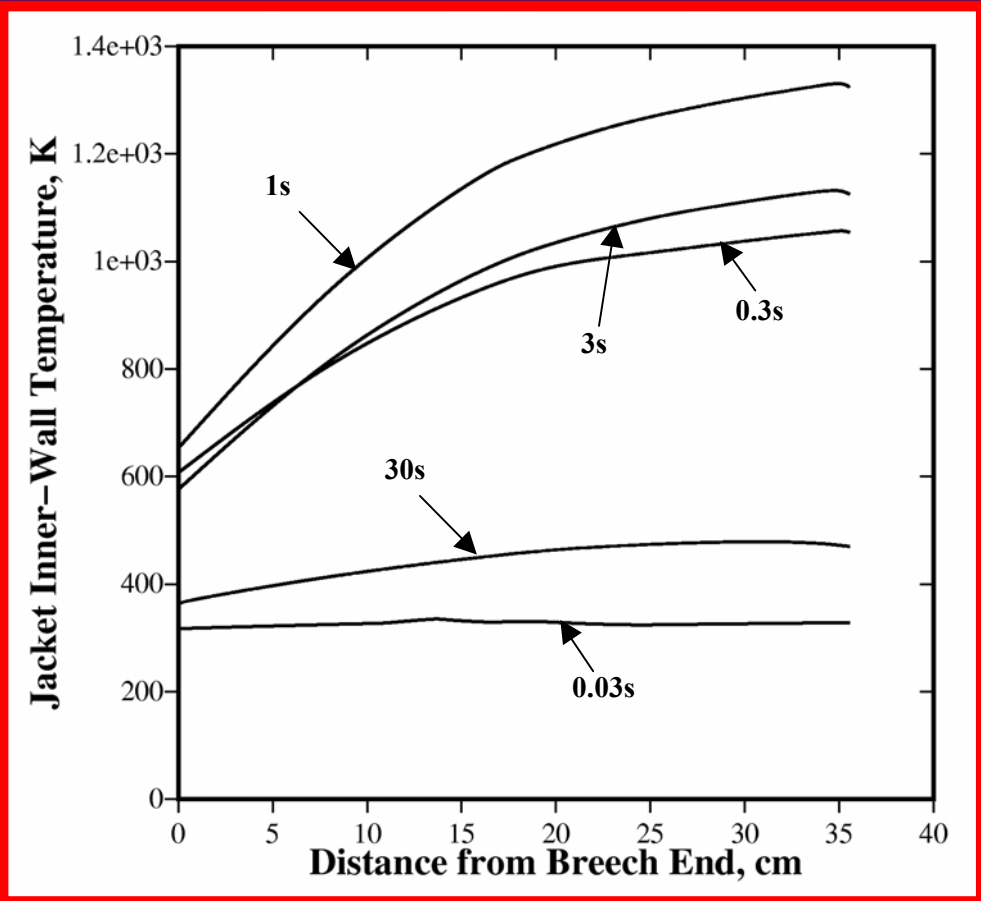


t=3.0s



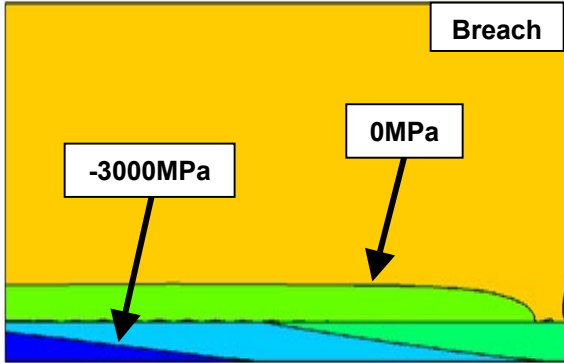
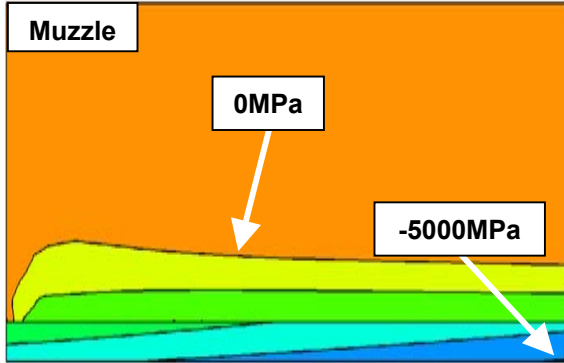
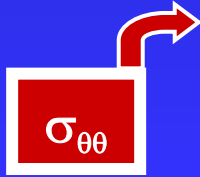
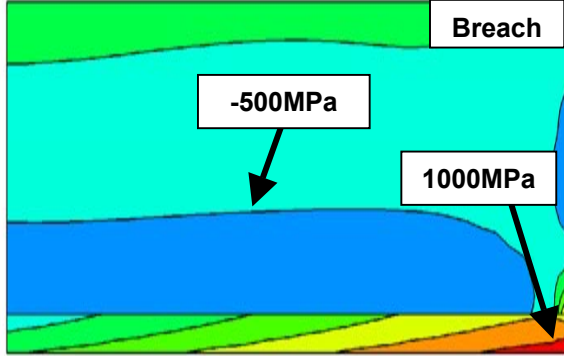
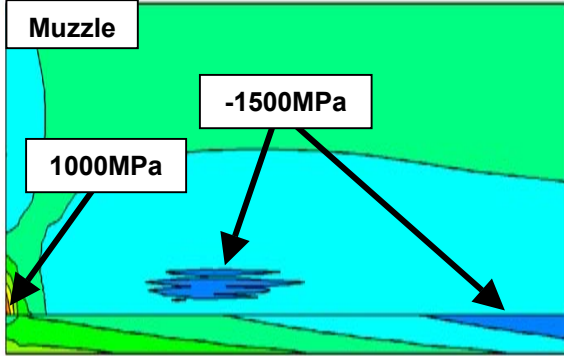
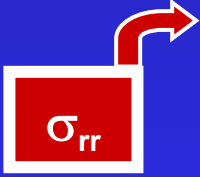
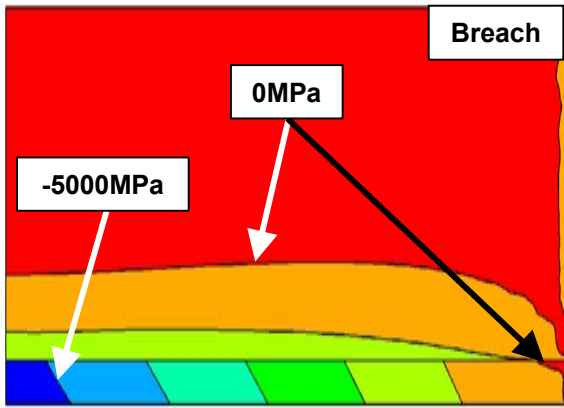
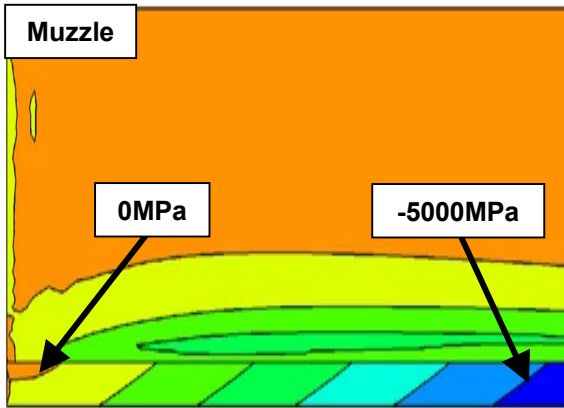
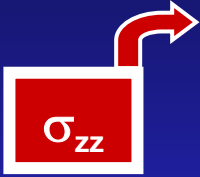
Single-shot Temperature

Max temperature in the jacket at lining/jacket contact surface is 1330K and occurs at 1 second after ignition



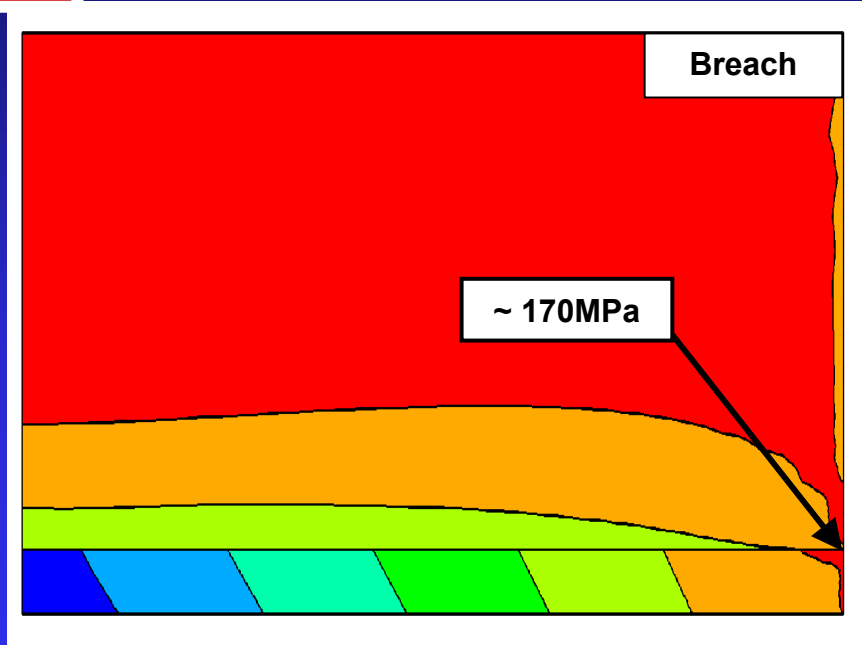
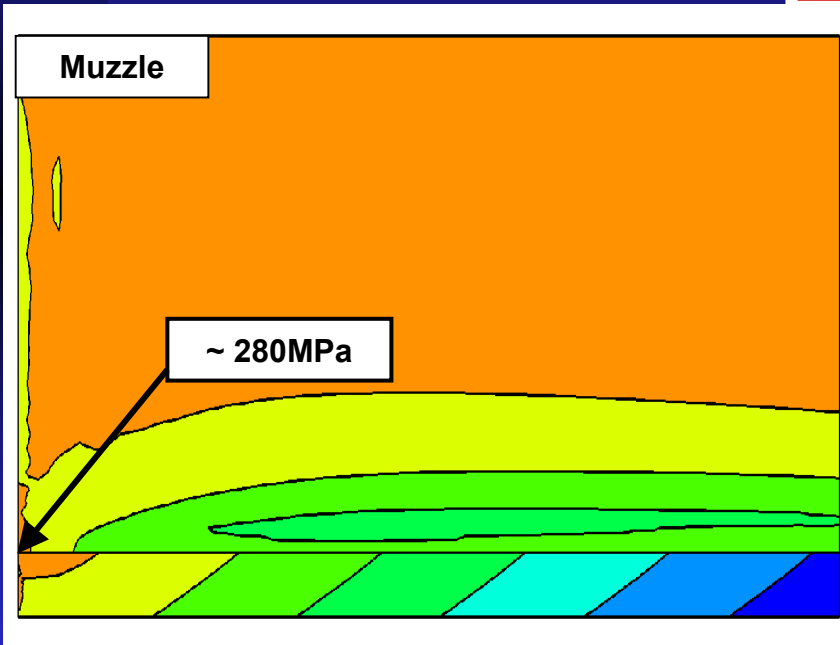
Single-shot Stress

Tensile Stress exists leading to finite probability for failure



Single-shot Stress

σ_{zz}



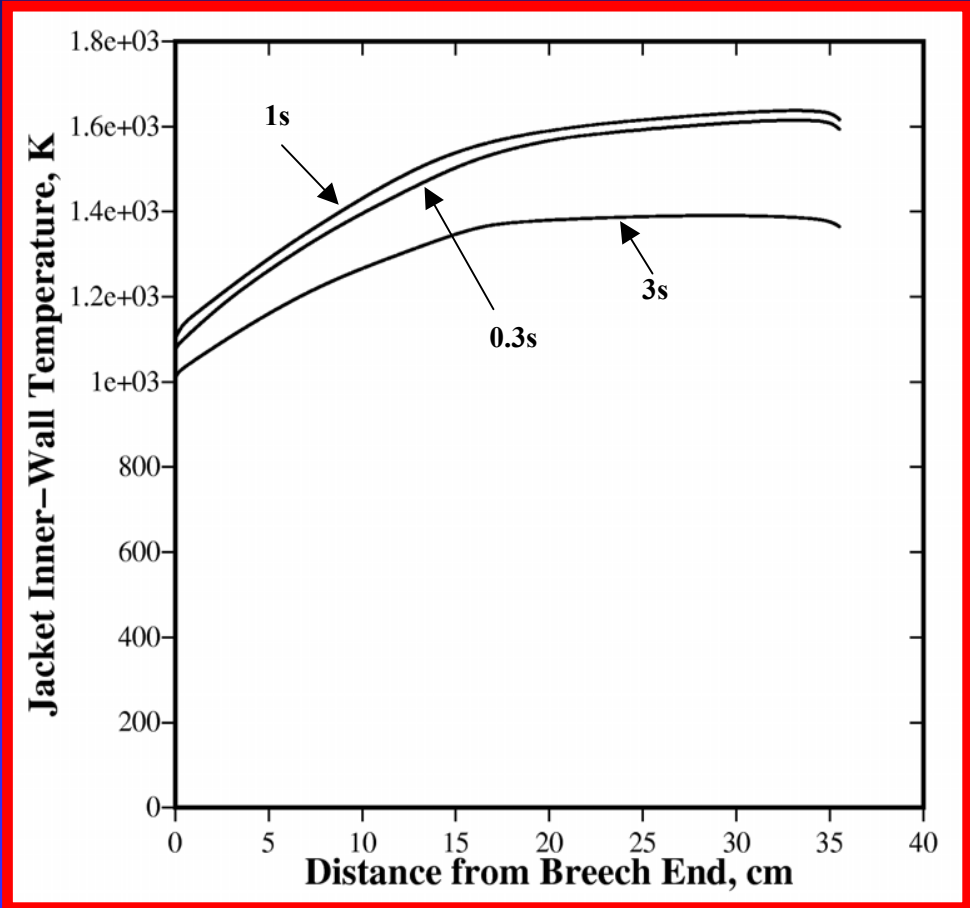
Muzzle region of the liner at the jacket interface on the barrel ends has highest stresses

Ten-round Burst Temperature

Burst temperature profile is periodic of single shot temperature profile

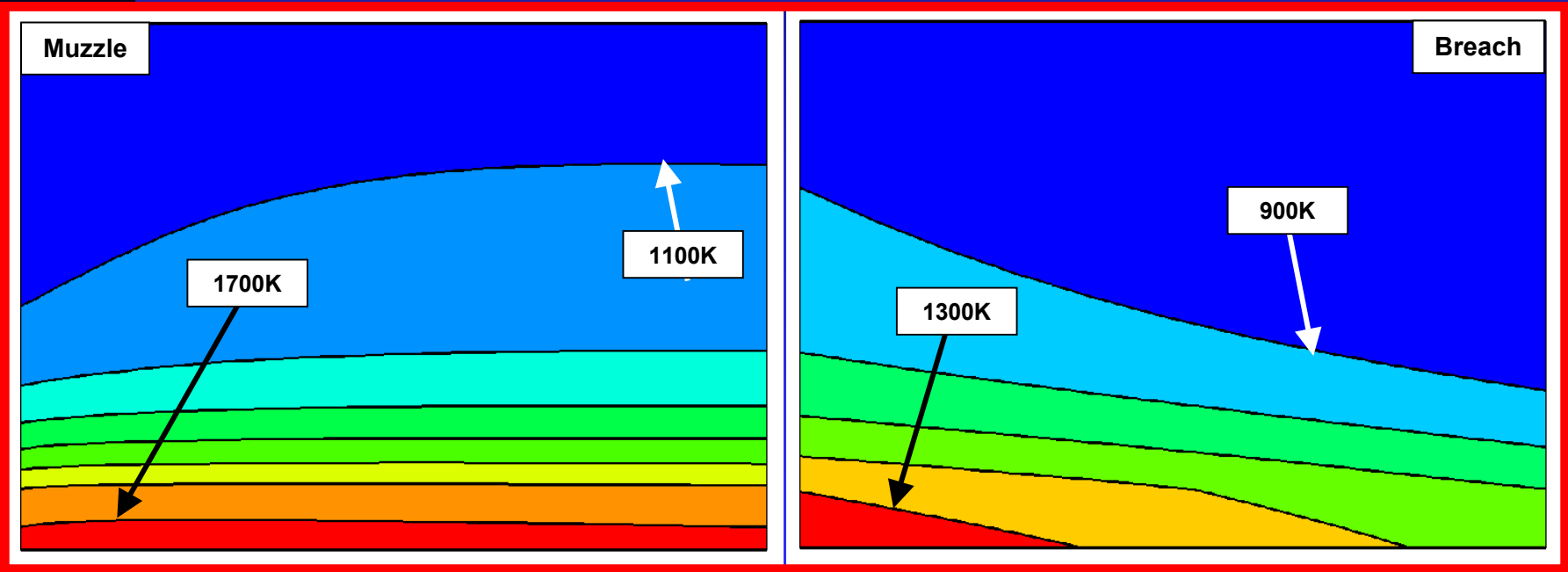
Max temperature in the jacket at lining/jacket contact surface is 1680K and occurs at 1 second after ignition

Ten-round burst temperature is as high as 350K more than single-shot



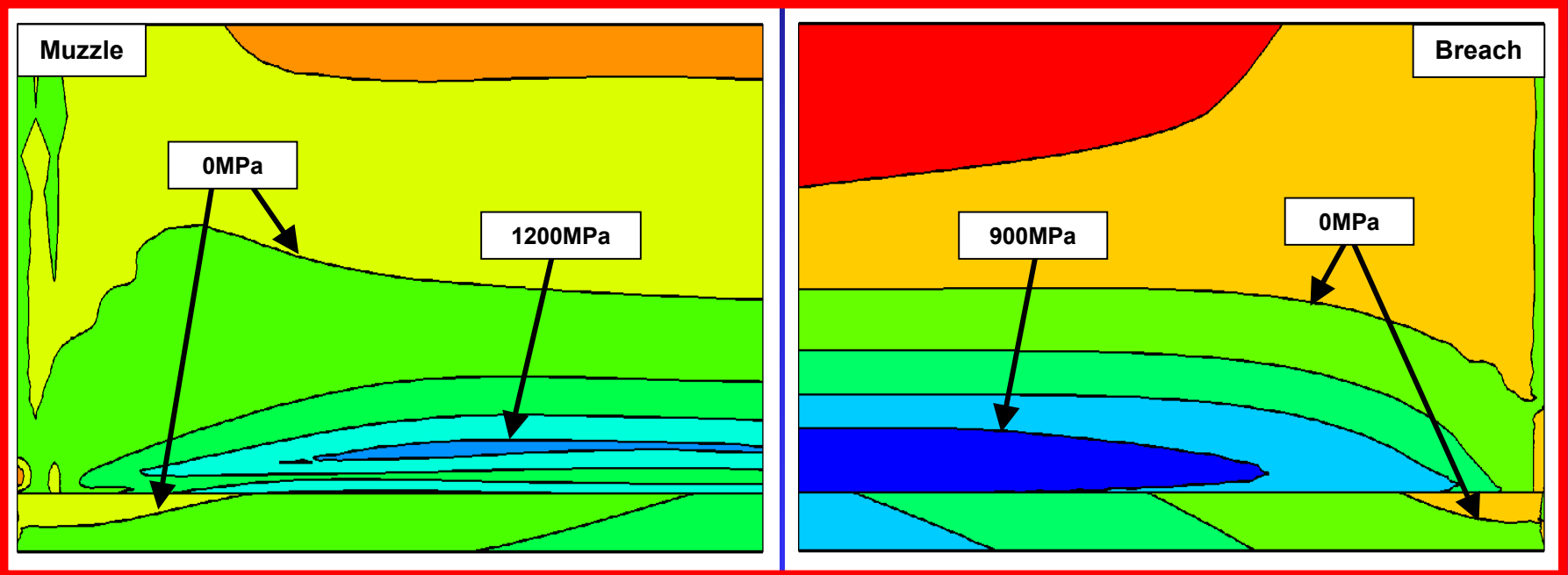
Ten-round Burst Temperature

At 1 second following the firing of the tenth round
(t=55seconds)



Ten-round Burst Stress

At 1 second following the firing of the tenth round
($t=55$ seconds)

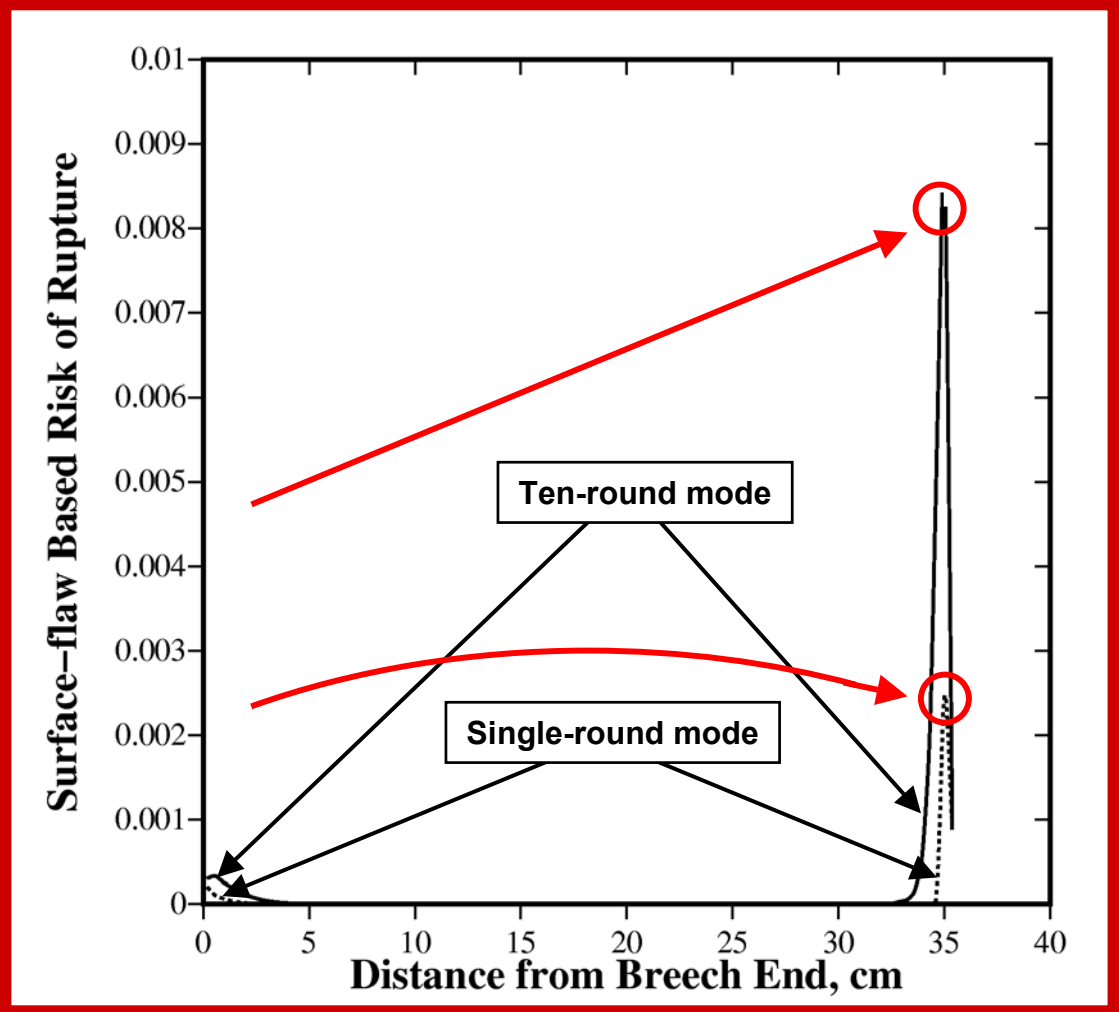


Risk of Rupture

Higher values are near barrel ends, lower values along the center length

0.00840 for ten-round mode

0.00220 for single-round mode



Summary of Reliability Analysis

- Thermal expansion the of steel jacket and development of tensile axial stresses upon firing cause lining to fail near the barrel ends
- Failure probability is over 300% higher for burst firing at 10 rounds/min than single-shot firing
- Extension of the steel jacket and increase in shrink-fit temperature may decrease lining failure probability

Part III

Effect of Lining

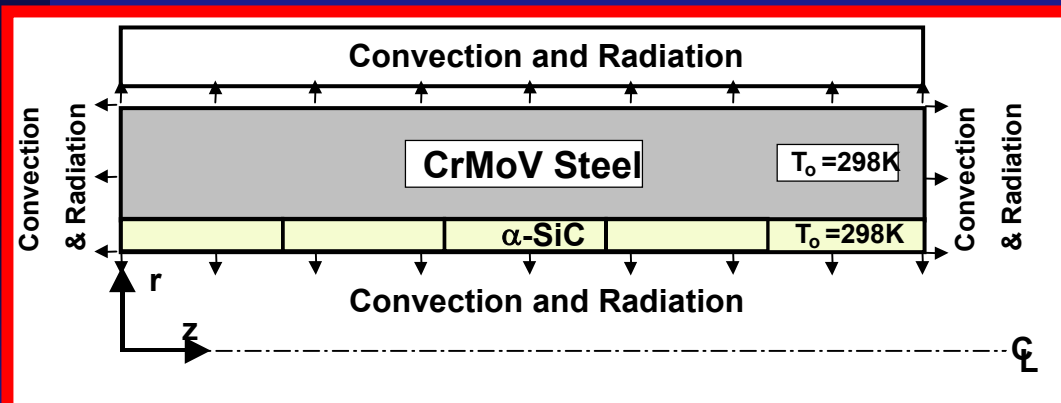
Segmentation on Hybrid

Ceramic/Steel Gun

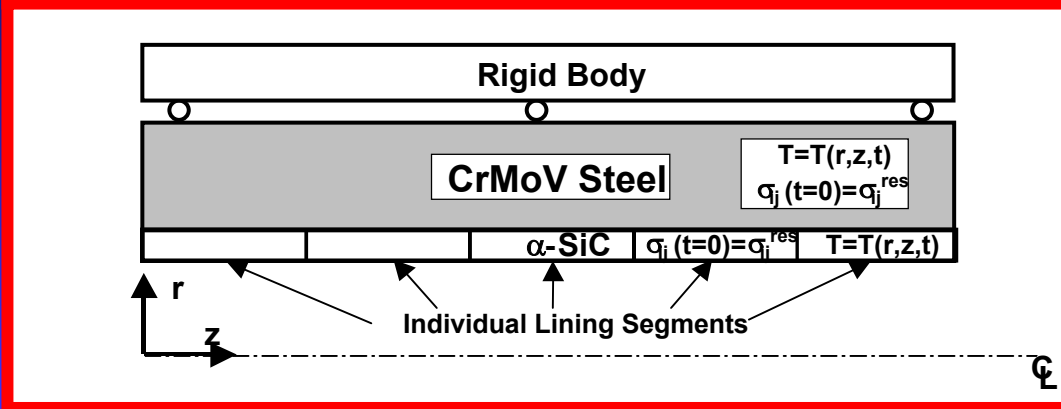
Barrels

Problem Formulation

- 2 step analysis now with segmentation
 - Transient heat transfer
 - Elastic-plastic mechanical stress

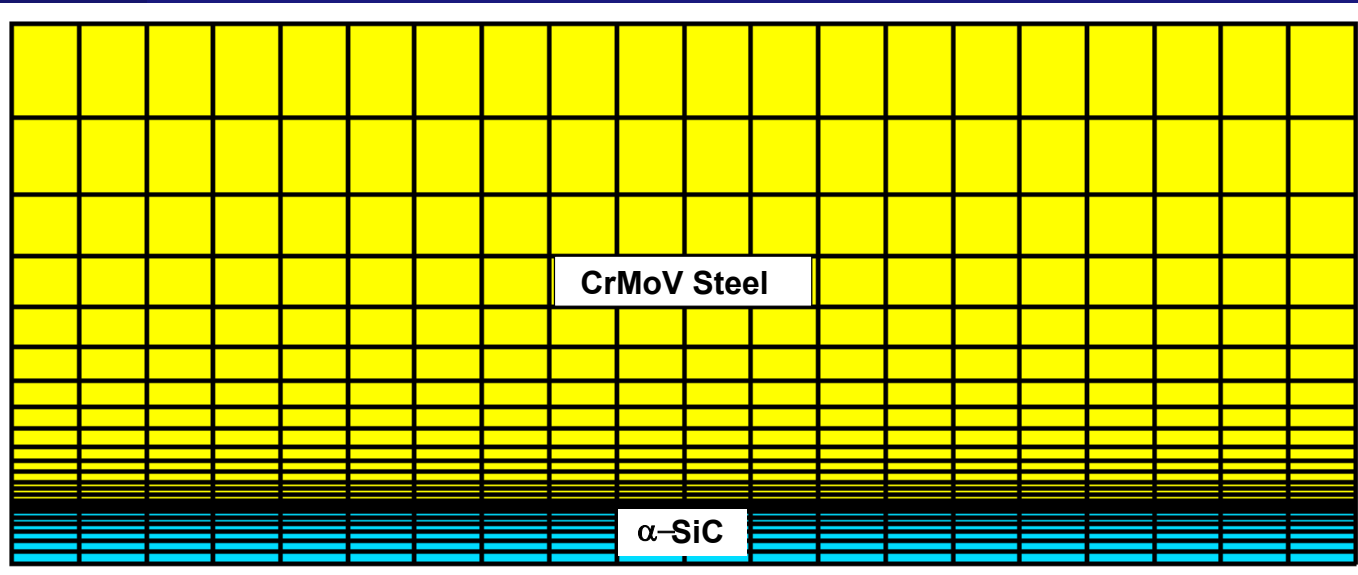


Temperature and heat transfer coefficient evolve temporally along inner barrel wall



Abaqus Mesh

Similar mesh to reliability analysis however segmentation is present

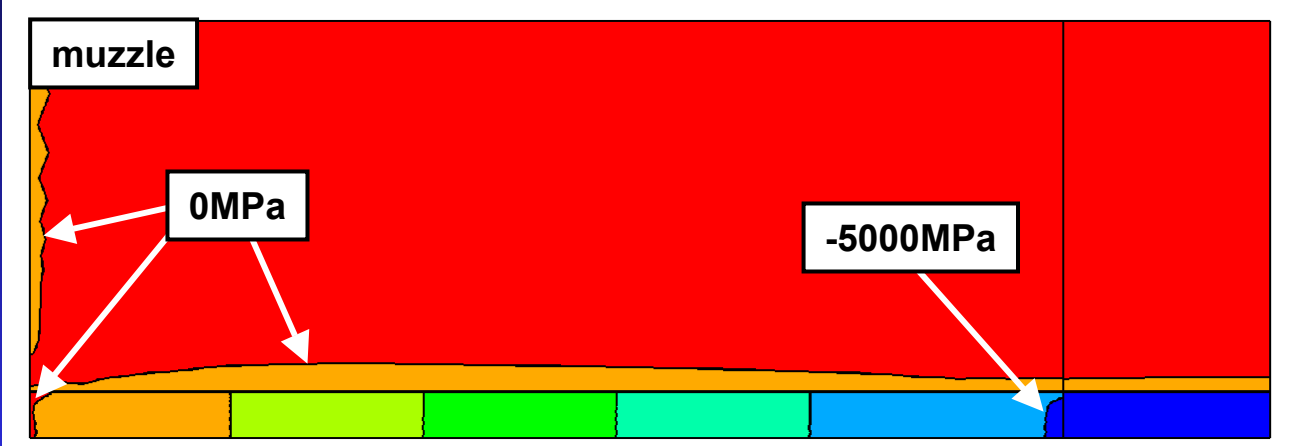


1 segment

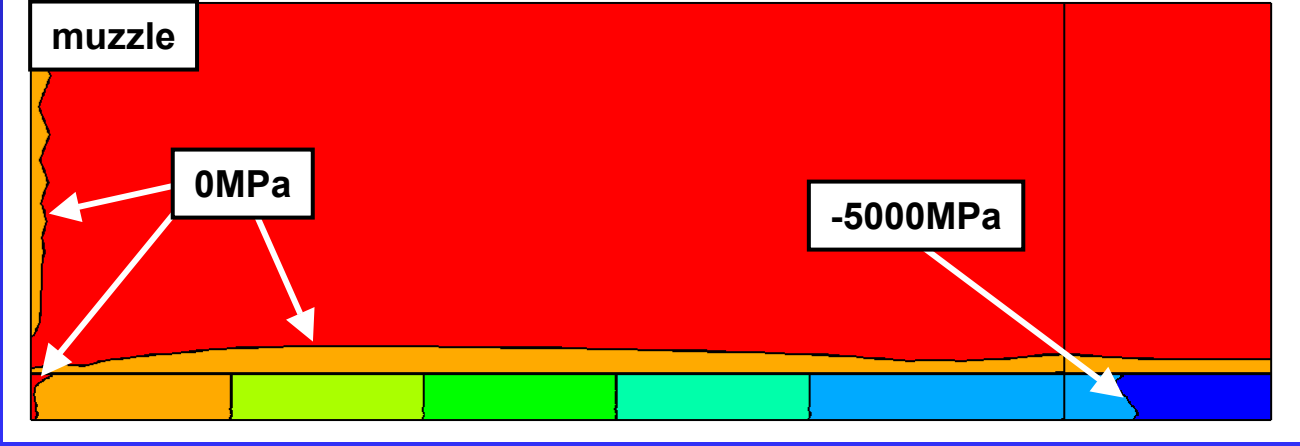
Contact elements used between individual ceramic segments

Shrink-fit Axial Stress

Single-piece

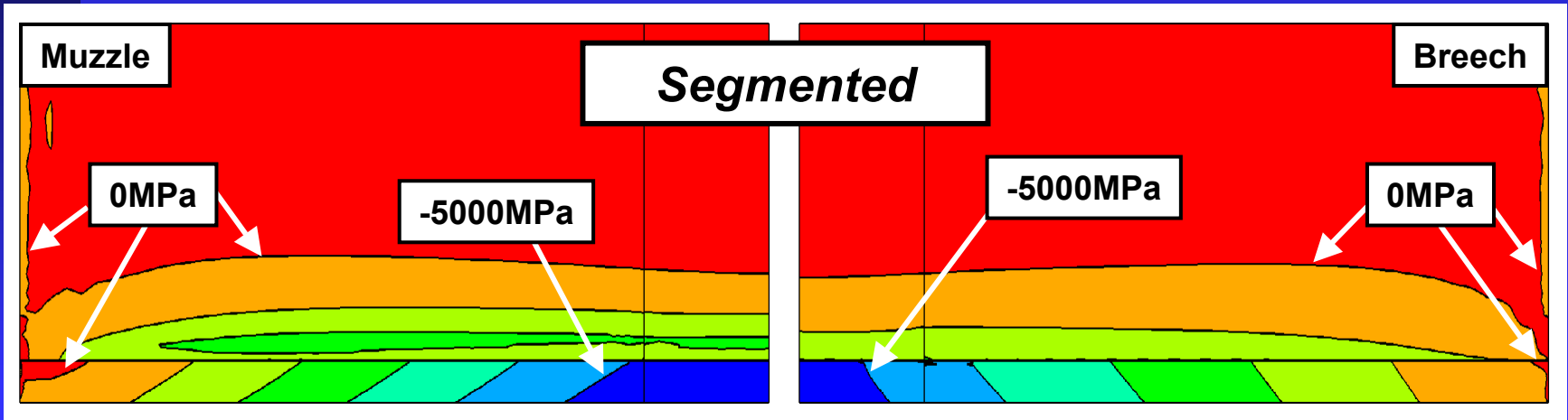
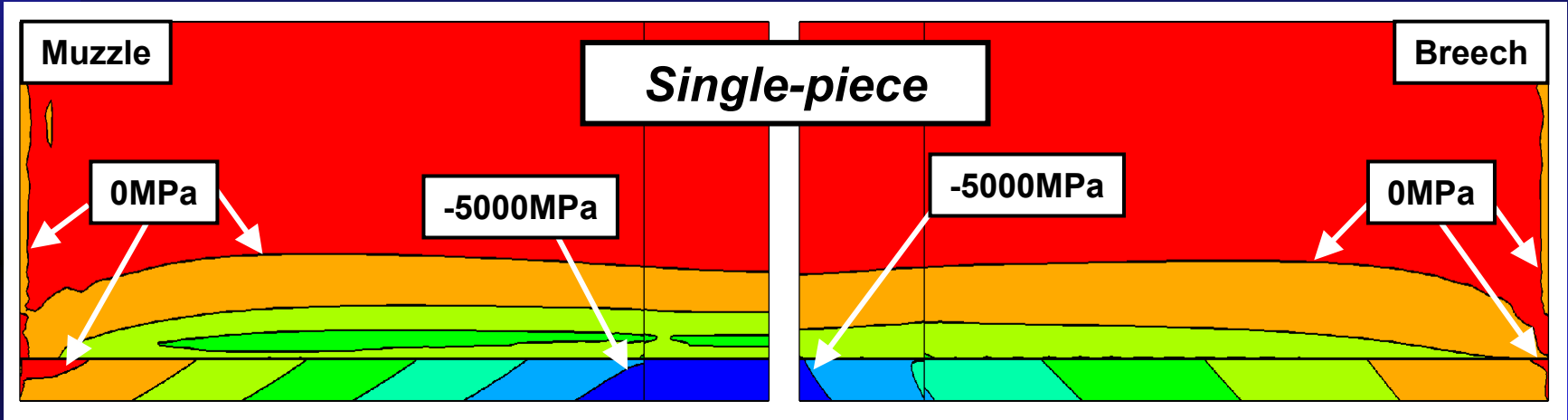


Segmented



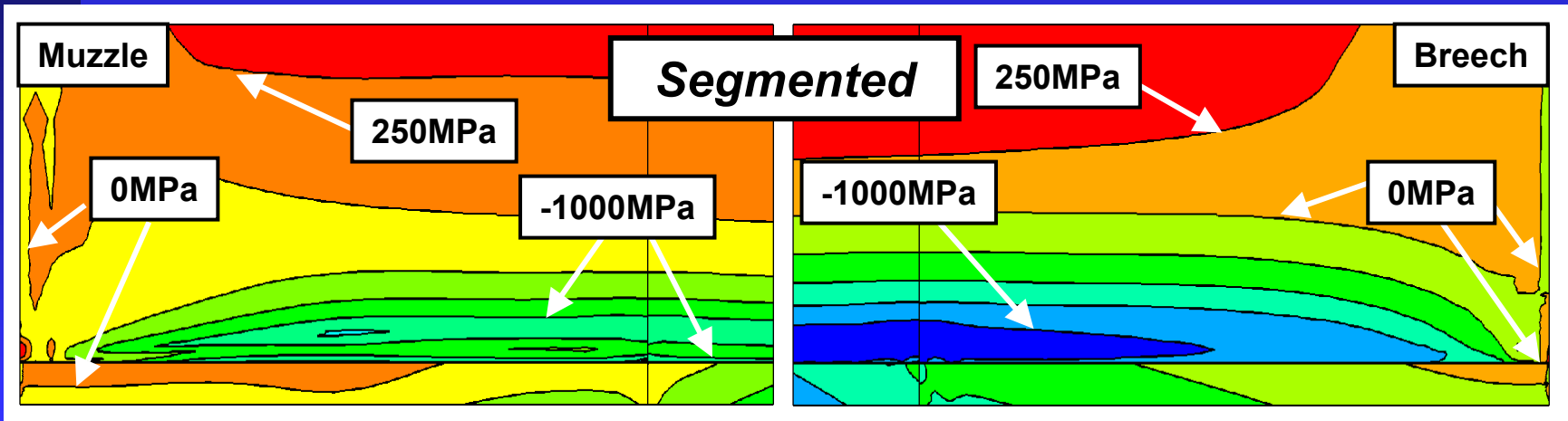
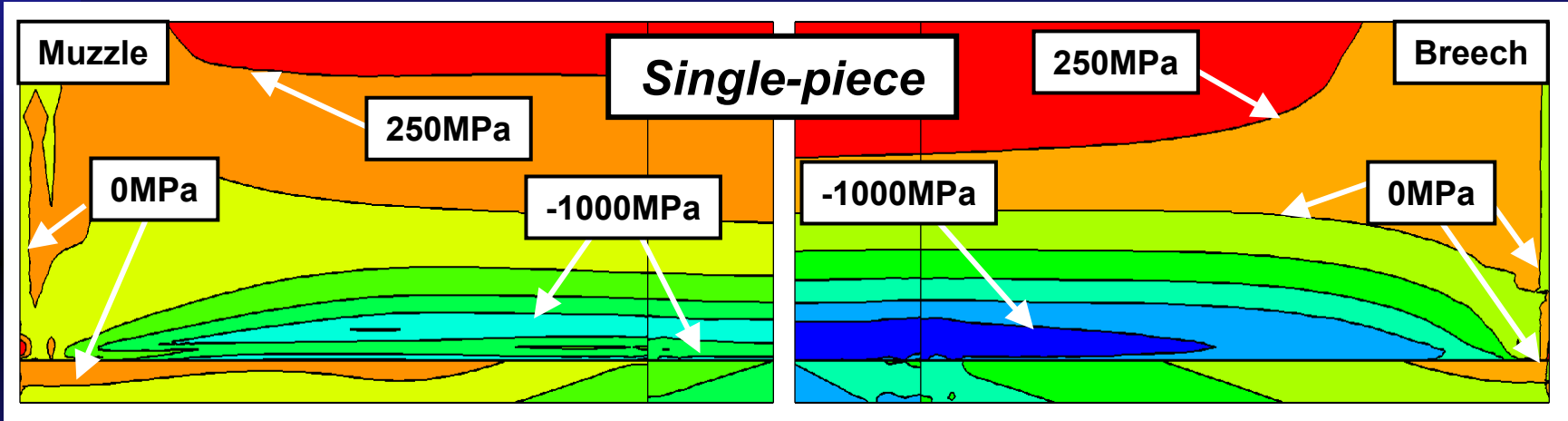
Single-shot Axial Stress

1 second following firing

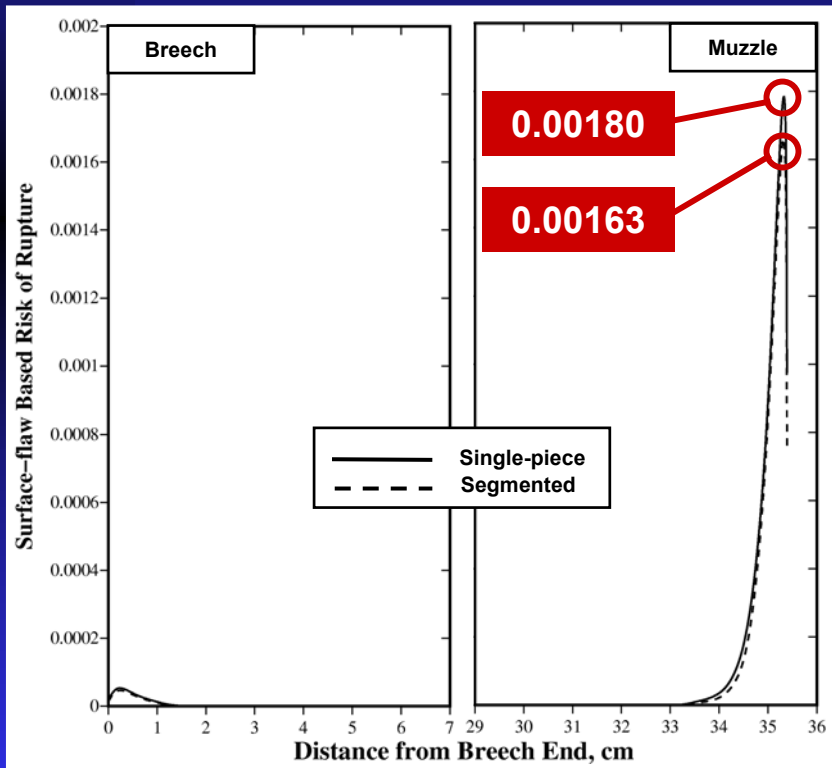


Burst-fired Axial Stress

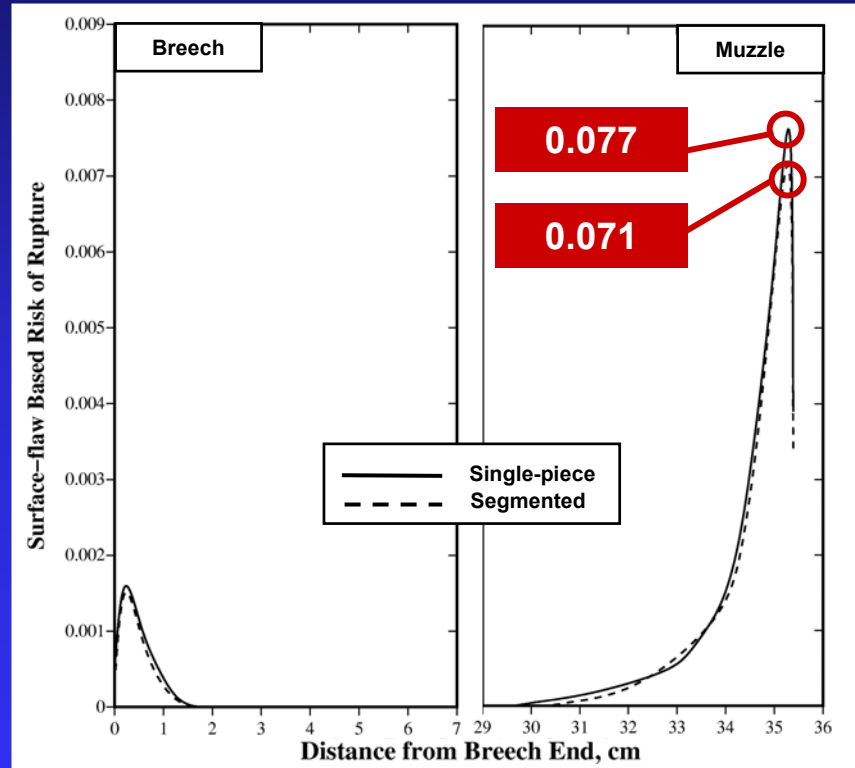
1 second following firing
of the last round



Risk of Rupture



Single-shot Mode



Burst-fired Mode

Failure Probability

- For Single-shot ballistic events:

- Single-piece $P_f = 0.0025$

- Segmented $P_f = 0.0023$

- Segmentation decreases P_f by $\sim 8\%$

- For Burst ballistic events

- Single-piece $P_f = 0.0121$

- Segmented $P_f = 0.0099$

- Segmentation decreases P_f by $\sim 18\%$

Summary of Segmentation Analysis

- Lining segmentation in fact reduces the lining failure probability
- Effects of lining segmentation impact burst events more than single-shot events
- 5 segment-barrels reduce lining failure probability by 18% for burst events with a 10 round/min firing rate

Structural Analysis Conclusions

- **The shrink-fit process causes the ceramic lining to develop a triaxial compressive residual stress but the relaxation of this stress at lining/jacket interface near barrel ends causes circumferential crack formation that promotes failure**
- **Steel jacket expansion and development of tensile axial stresses upon firing cause the lining to fail near the barrel ends**
 - **Failure probability is over 300% higher for burst firing at 10 rounds/min than single-shot firing**
 - **Extending the steel jacket and increasing the shrink-fit temperature may decrease lining failure probability**
- **Lining segmentation reduces the lining failure probability particularly in the case when 5 individual segments are utilized**
 - **Burst events show a failure probability reduction of 18% with segmentation, while single-shot failure probability reduces only by 8%**

END